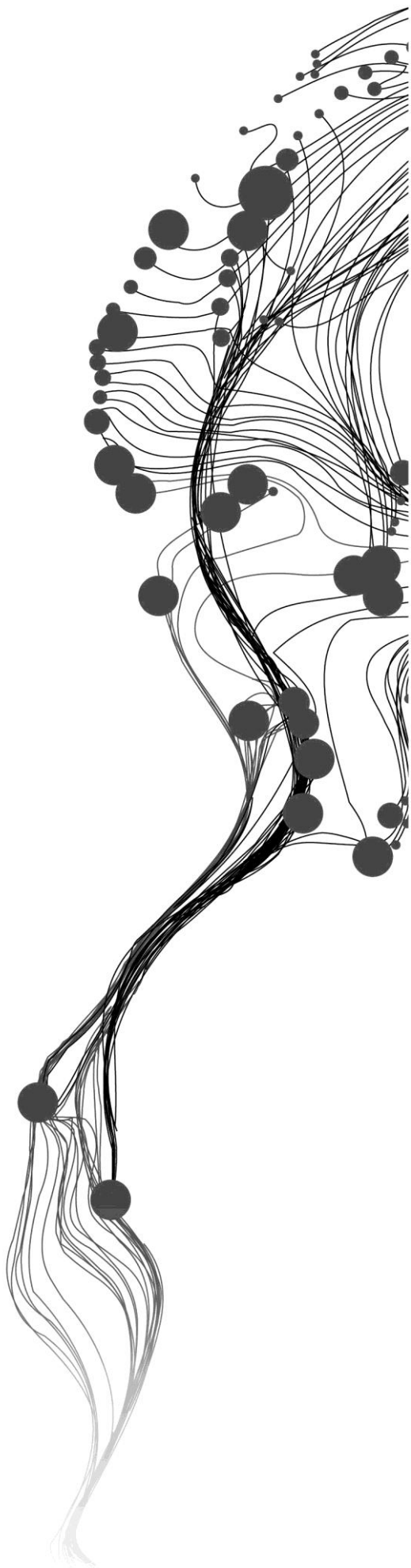


# **SIMULATION OF GROUNDWATER RECHARGE IN THE SARDON CATCHMENT, SPAIN**

CÉSAR CISNEROS  
MARCH, 2011

SUPERVISORS:  
MSc. Ir. Gabriel Parodi  
Dr. Ir. Christiaan van der Tol



# **SIMULATION OF GROUNDWATER RECHARGE IN THE SARDON CATCHMENT, SPAIN**

**CÉSAR CISNEROS**

Enschede, The Netherlands, March, 2011

Thesis submitted to the Faculty of Geo-Information Science and Earth Observation of the University of Twente in partial fulfilment of the requirements for the degree of Master of Science in Geo-information Science and Earth Observation.

Specialization: Water Resources and Environmental Management

**SUPERVISORS:**

MSc. Ir. Gabriel Parodi

Dr. Ir. Christiaan van der Tol

**THESIS ASSESSMENT BOARD:**

Dr. Ir. M.W. Lubczynski (Chairman)

Prof. O. Batelaan (External Examiner, Brussel University - Dept. of Hydrology and Hydraulic engineering)

#### DISCLAIMER

This document describes work undertaken as part of a programme of study at the Faculty of Geo-Information Science and Earth Observation of the University of Twente. All views and opinions expressed therein remain the sole responsibility of the author, and do not necessarily represent those of the Faculty.

## ABSTRACT

---

Diverse techniques are available to quantify ground water recharge in the semi arid catchment of Sardon River. Methods as chloride mass balance or numerical models that solve Richard's equations have been implemented. However, since assessment of groundwater recharge is an iterative process that comprises refinement of estimates as additional data are gathered, a different approach using INFIL3.0, a distributed water-balance model for the unsaturated zone, has been applied in order to estimate groundwater recharge.

Computer code of INFIL3.0 developed for semiarid areas has been adapted to the data availability of Sardon Catchment. Meteorological information, thematic maps and field observations are processed using GIS techniques to use as input for the model. Due to the absence of streamflow data for calibration, evaluation of the model by comparing values of evapotranspiration calculated at the eddy tower and comparing the trend of soil moisture in a soil profile are proposed as surrogate.

For the period 2007-2008, with an average precipitation of 515 mm/year, the average annual ground water recharge estimated in the simulation is 72mm/year. This value is equivalent to 14% RF (percentage of rainfall). The spatial distribution showed higher groundwater recharge values located over stream channels and close to outcrops >40%RF and very low groundwater recharge values for areas close to massive and fractured granite. The results of previous studies are: for steady state modelling MODFLOW 11%RF (Lubczynski and Gurwin, 2005) and 12%RF (Ruwan Rajapakse, 2009); those averaged from simulations with pyEarth1D 20%RF (Ruwan Rajapakse, 2009) and Earth1D 18%RF (Uria Cornejo, 2000); and averaged values obtained by Chloride mass balance method 10.5%RF (Ruwan Rajapakse, 2009). These values show a similarity compared to the present study results.

Despite these values of recharge are numerically comparables with those obtained from other methods as chloride mass balance and pyEarth1D, calibration and configuration of surface routing parameters are suggested in order to increase the confidence of these results.

Keywords: Sardon, model, groundwater, recharge, INFIL, semi arid

## ACKNOWLEDGEMENTS

---

I would like to thank my family who always have encouraged me to move forward in my goals.

Thanks to ITC for sponsoring this Master of Science in The Netherlands, and also to CLAS for its support from Bolivia.

I would like to express my gratitude to all ITC staff, particularly to my supervisors Gabriel Parodi and Christiaan van der Tol for their guidance, suggestions and help during my research time. Thank you for your valuable advices.

I also want to express my gratitude to the research group in the Sardon Catchment especially to Alain, Enrico, Leonardo, and Tanvir, thanks for all the comments and assistance during this period. I extend my gratitude to Dr. Boudewijn de Smeth for his guidance throughout laboratory stage.

Thanks to all my colleagues in ITC, and friends from WREM department, especially the Campo Charro group.

Last but not least, my grateful to the Latin American community in ITC, who helped and support me during this great days in Enschede..

*This thesis is dedicated to my Mom.*

---

# TABLE OF CONTENTS

---

Abstract .....	1
Acknowledgements .....	2
List of figures .....	ii
List of tables .....	iii
1. INTRODUCTION.....	1
1.1. Background.....	1
1.2. Problem definition .....	2
1.3. Research Objectives .....	2
1.4. Research Questions.....	2
1.5. Methodology .....	2
2. LITERATURE REVIEW.....	5
2.1. Description of the study area .....	5
3. MODEL DESCRIPTION .....	7
3.1. Model INFIL3.0 .....	7
3.2. Spatial discretization of INFIL3.0.....	7
3.3. Spatial distribution of Daily Climate Data .....	9
3.4. Potential Evapotranspiration.....	9
3.5. Infiltration, Drainage Evapotranspiration, and Runoff.....	10
4. MATERIALS AND METHODS .....	13
4.1. Data requirements for INFIL3.0 model.....	13
4.2. Climate data .....	13
4.3. GIS data .....	16
4.4. Digital Elevation Model - DEM.....	17
4.5. Soil Map .....	19
4.6. Bedrock Map.....	23
4.7. Vegetation Map.....	24
4.8. Model Set up and Initial conditions .....	28
4.9. Evaluation of the Model .....	28
5. RESULTS AND DISCUSSION .....	29
5.1. Data Aquisition.....	29
5.2. Model simulations .....	37
5.3. Evaluation of the model.....	37
5.4. Results of model simulation .....	41
6. CONCLUSIONS AND RECOMENDATIONS.....	45
List of references .....	47
APPENDIX A.....	49
APPENDIX B .....	50
APPENDIX C.....	53
APPENDIX D .....	55

## LIST OF FIGURES

---

Figure 1. Study area Sardon catchment, Spain, after-(Lubczynski and Gurwin, 2005).....	5
Figure 2. Average monthly rainfall and temperature variation in a year during the period 2003-2008, after (Ruwan Rajapakse, 2009) .....	6
Figure 3. Horizontal discretization of a basin in INFIL3.0 (U.S.G.S., 2008).....	8
Figure 4. Vertical discretization for INFIL3.0 model (U.S.G.S., 2008).....	8
Figure 5. Data Requirements for INFIL3.0 model.....	13
Figure 6. Cumulative precipitations of Trabadillo Station vs. Villarmuerto Station .....	14
Figure 7. Location of ADAS stations in Sardon Catchment - after (Lubczynski and Gurwin, 2005).....	15
Figure 8. Example of Geospatial Watershed Characteristic File Variables.....	18
Figure 9. Soil samples locations .....	19
Figure 10. Locations of infiltration tests.....	21
Figure 11. Generic landforms associated to soil depth.....	22
Figure 12. Soil depth map flowchart .....	23
Figure 13. Sample pixel with its percentage of vegetation classes.....	25
Figure 14. Vertical discretization for the species <i>Q. Ilex</i> & <i>Q. Pyrenaica</i> .....	26
Figure 15. Water stress coefficient, $K_s$ .....	27
Figure 16. Curves of adjusted parameters $\alpha$ , $\beta$ .....	28
Figure 17. Monthly Rainfall in Trabadillo station showing warming up and simulation periods. ....	29
Figure 18. Potential evapotranspiration calculated with modified Priestley-Taylor equation by INFIL3.0 model.....	30
Figure 19. Particle size distribution in the point TBSTA30 according to depth.....	31
Figure 20. Particle size distribution in the point TREMSS according to depth.....	31
Figure 21. Soil depth map .....	33
Figure 22. Soil depth map .....	33
Figure 23. Visual evaluation of soil depth map using Orthophotography. ....	35
Figure 24. Bedrock map after (Tesfai, 2000).....	35
Figure 25. Vegetation Map in percentage of tree coverage per grid cell. ....	36
Figure 26. Fluxes precipitation and evapotranspiration, 2010 determined in the tower .....	38
Figure 27. Fluxes precipitation and evapotranspiration, 2008 calculated by INFIL3.0 .....	38
Figure 28. Comparing cumulative fluxes for precipitation and actual evapotranspiration for the years 2008 (left) and 2010 (right).....	39
Figure 29. Soil moisture profiles. Thick lines represent values of soil moisture converted from matric potential sensor installed under <i>Q. Pyrenaica</i> tree, and segmented line represent values simulated from the model for corresponding pixel location.....	40
Figure 30. Soil water content simulated and calculated from matric potential sensor at 25 (cm).....	41
Figure 31. Root zone mass balance .....	41
Figure 32. Recharge Map (mm/year) .....	42
Figure 33. Recharge in percentage of rainfall for the period 2007 to 2008 .....	43

## LIST OF TABLES

---

Table 1. Climate Data Requirements for INFIL3.0 model.....	13
Table 2. GIS Data Requirements for INFIL3.0 model.....	16
Table 3. Grid cell size for the input maps .....	17
Table 4. Monthly Atmospheric Parameters.....	29
Table 5. Summary of Soil Hydraulic properties derived from different laboratory and field methods.....	32
Table 6. Soil Classes with hydraulic properties.....	32
Table 7. Hydraulic properties for the bedrock.....	36
Table 8. Parameters that control surface water routine.....	37
Table 9. Values of recharge calculated in previous studies .....	44
Table 10. Example of segmentation of vegetation classes.....	53
Table 11. Sample of root density estimation.....	53



# 1. INTRODUCTION

## 1.1. Background

Increasing demands on limited water supplies in semiarid and arid regions result in a critical drawdown of groundwater levels. Water scarcity will become more critical in the future as population growth in (semi-) arid regions surpasses that in more humid settings (Scanlon, et al., 2006). Hence, sustainable management of groundwater resources requires accurate estimations of groundwater recharge.

Groundwater recharge can be defined in a broad sense as ‘the addition of water to a groundwater reservoir’ (Vrba and Lipponen, 2007). The issue of recharge assessment has been an object of many research publications. An outstanding collection is in the special issue of *Hydrogeology Journal* no. 1 from 2002 (Scanlon, et al., 2002). This issue highlights a deep overview of the recharge methods advising on the selection criteria for different hydrological conditions.

Although many methods to estimate ground-water recharge have been already applied in Sardon catchment, a different method not yet tested is the distributed watershed modeling. This method allows the determination of temporally distributed net infiltration and recharge at locations distributed throughout a watershed (U.S.G.S., 2008). Although distributed groundwater modeling approaches are more data demanding (Sanford, 2002), they also provide more reliable and more complex recharge distribution (Stasko, et al., 2008).

One of such watershed model is the INFIL computer code, this is a distributed-parameter, deterministic precipitation-runoff and net-infiltration water-balance simulation model (U.S.G.S., 2008). INFIL was initially developed for application to the Yucca Mountain area of Nevada and was subsequently extended for an application in the larger Death Valley region of Nevada and California within which Yucca Mountain is located (U.S.G.S., 2008). The model also has been applied to estimate recharge for the area near Joshua Tree, California, by Nishikawa and others (2004), the San Gorgonio Pass area, Riverside County, California, by Rewis and others (2006), and the Big Bear Lake area, California (U.S.G.S., 2008).

The semi-arid catchment of Sardon which is located in Salamanca province, central part of Spain present similar semi-arid conditions to those which INFIL model has been applied. The Sardon catchment has been used for ITC experimental studies since 1996. Many studies have been carried out in respect ground water recharge and numerical modeling (Berhe, 2010; Lubczynski and Gurwin, 2005; Ruwan Rajapakse, 2009; Shakya, 2001; Uria Cornejo, 2000).

Those previous studies carried out in the Sardon catchment emphasize the uncertainties presents in the ground water modeling due to the complexity of the flow regimes and spatial-temporal flux variability. Two of the main flux uncertainties are evapotranspiration from groundwater (ET<sub>g</sub>) and Recharge (R) both of them are inputs for groundwater modeling.

The development of INFIL model could help to manage the irregular spatiotemporal distribution of recharge present in the Sardon catchment, and could be an additional contribution in order to enhance confidence in recharge estimates.

## 1.2. Problem definition

Previous MSc Thesis dealing with recharge are: The assessment of groundwater recharge using remote sensing and GIS applications and using EARTH-1D model by Uria Cornejo (2000), Numerical groundwater flow and solute transport modeling Ruwan Rajapakse (2009), the semi-distributed recharge model pyEARTH-2D applied to estimate of spatially distributed recharge by Berhe (2010),

These previous studies reflect the evolution from one dimensional models as Earth1D, which don't consider the fluctuations caused by horizontal saturated flow or the areal distribution (Uria Cornejo, 2000), to two dimensional model pyEarth 2D. None of these models has been compared with an independent method for Sardon.

Since assessment of groundwater recharge is an iterative process that comprises refinement of estimates as additional data are gathered, the application of a numerical 2.5 dimensional model as INFIL could be a new and valuable contribution for the estimation of groundwater recharge in the Sardon catchment.

## 1.3. Research Objectives

The main objective is to estimate groundwater recharge in the Sardon Catchment using the Spatio-temporal distributed water balance model INFIL3.0, in the period from January 2007 to Dec 2008.

The specific objectives are:

- To define a procedure based on GIS and fieldwork observations to achieve the spatial discretization of the inputs (soil, vegetation, watershed properties) of the INFIL3.0 model.
- To estimate the soil depth by using the geomorphologic map and the high resolution DEM of the Sardon catchment.
- To evaluate the simulation of ground water recharge from INFIL3.0 model in the Sardon Catchment.
- To compare values of groundwater recharge calculated with INFIL3.0 in the Sardon Catchment with previous studies.

## 1.4. Research Questions

- Which GIS methods allow obtaining the input maps that the INFIL3.0 model requires?
- What is the spatial distribution of soil depth in the catchment?
- Which is the spatial distribution of groundwater recharge over the Sardon catchment for the period 2007 - 2008?
- Is the groundwater recharge estimated by INFIL3.0 comparable to the estimated values of previous studies?

## 1.5. Methodology

The methodological steps for the fulfilling of the research objectives will be carried out in three stages: pre-fieldwork, fieldwork, post-fieldwork, modeling, and discussion of results.

### **1.5.1. Pre-fieldwork stage**

The pre-field work stage is focused in the preparation of the activities which facilitate the field work and the development of the project at all. For that reason was necessary to review the documentation related to the study area, model, previous studies, and data availability. This stage includes the following activities.

- Literature review
- Exploratory analysis of INFIL3.0
- Determining the input data requirement of INFIL3.0.
- Localization of sites to take samples and to make field experiments.
- Field work schedule.

### **1.5.2. Fieldwork stage**

The activities conducted in this stage will include:

- Area recognizing.
- Downloading Meteorological information from ADAS stations
- Verification of the selected locations for soil sampling.
- Collecting data:
  - Soil samples to analyze hydrological properties. Samples collected in two ways core (undisturbed) soil samples and bags (disturbed) soil samples.
  - Soil depth measurements.
  - Infiltration tests to characterize soils in relation to position..

### **1.5.3. Lab analysis stage**

Consists on:

- Laboratory analysis:
  - Permeameter (Saturated conductivity) for core samples.
  - Textural analysis (Particle size discrimination) for bags soil samples.
  - Analysis of infiltration tests

### **1.5.4. Modeling, and discussion of results**

This stage's activities were:

- Preparation of input files for INFIL3.0 model.
- Develop of INFIL3.0 model
- Evaluation of INFIL3.0 model.
- Analysis of results.
- Elaboration of the final document for its submission.

### **1.5.5. Thesis Outline**

This written report has been organized in 6 Chapters as follow:

Chapter 1 describes the problem statement and research objectives proposed.

Chapter 2 gives a brief description of the study area.

Chapter 3 explains INFIL3.0 model equations and concepts.

Chapter 4 contains the methodology used to develop INFIL3.0 model in the study area.

Chapter 5 analyzes the results obtained from the simulation.

Chapter 6 formulates the conclusion and recommendations of this research.

## 2. LITERATURE REVIEW

### 2.1. Description of the study area

#### 2.1.1. Location

The Sardon River catchment is located in the western part of the Iberian Peninsula, about 50Km from the city of Salamanca (Figure 1), between 6°07' and 6°13' W and 41°01' and 41°08' N. The size of the catchment is ~80 km<sup>2</sup> characterized by well defined physical boundaries, low human population and therefore low human impact, semi-arid conditions, typical fractured granite rocks and land cover with standard hard rock hydrology problems(W. Lubczynski and Gurwin, 2005).

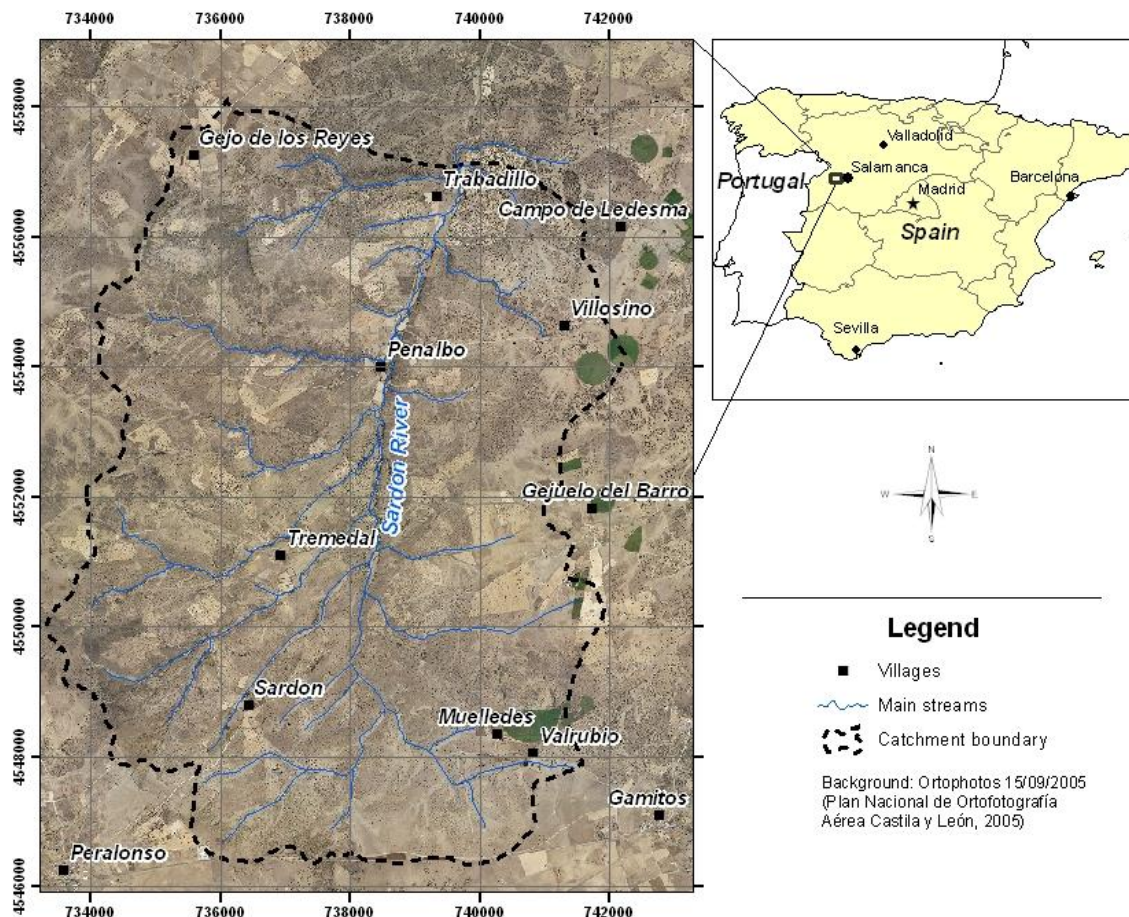


Figure 1. Study area Sardon catchment, Spain, after-(Lubczynski and Gurwin, 2005)

#### 2.1.2. Climate

The climate in the study area is semi-arid and is typical for the central part of the Iberian Peninsula. The long-term 23-years mean rainfall, estimated on the base of six Spanish Meteorological Institute rain gauges located in the surroundings of the study area was ~500 mm/yr. The warmest and the driest months in the study area are July and August when the average temperature is ~22 °C, potential evapotranspiration

(PET) is on average  $\sim 5$  mm/d and rainfall is less than 20 mm/month. The coldest months are January and February with an average temperature  $\sim 5$  °C, the wettest November and December with rainfall above 100 mm/month and the lowest PET is in December and January, on average  $\sim 0.5$  mm/d (Lubczynski and Gurwin, 2005). These considerations are important because in semiarid conditions the temporal distribution of recharge is irregular and that fact should be expressed in the results of INFIL simulations, in Figure 2 the monthly variations of rainfall during the year.

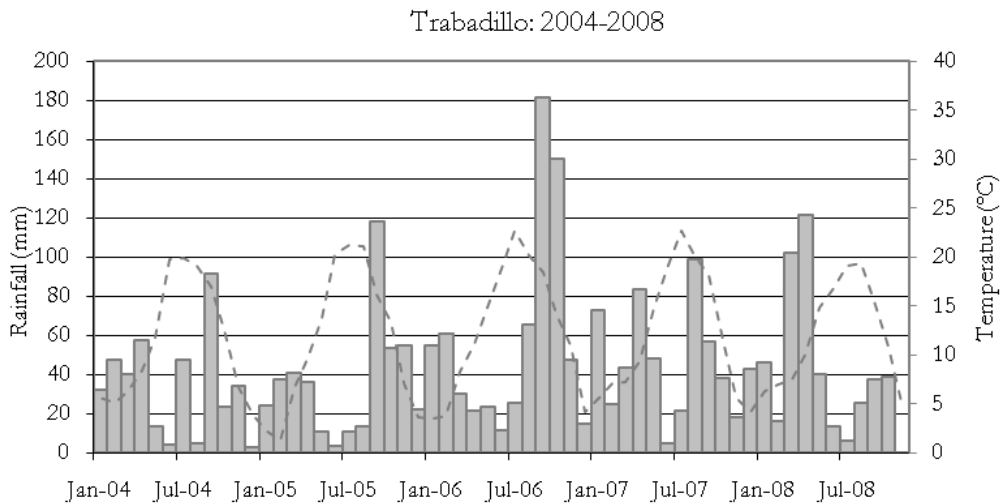


Figure 2. Average monthly rainfall and temperature variation in a year during the period 2003-2008, after (Ruwan Rajapakse, 2009)

### 2.1.3. Land cover

The land cover in the study area is characterized by natural woody-shrub vegetation. The area is used mainly for pasture because the soils contain large proportions of weathered granite, which make them generally unsuitable for agriculture. There are only two types of tree species in the study area: evergreen oak *Quercus ilex*, broad-leaved deciduous oak *Quercus pyrenaica*. Further, there are grasses and abundant shrub *Cytisus scoparius* vegetation also known as Scotch Broom (Lubczynski and Gurwin, 2005). The information about vegetation cover and root depth is important as they manage the horizontal and vertical discretization in the model.

### 2.1.4. Drainage

At regional scale all major rivers including Sardon River; drain into Tormes River, a perennial river, which has a dam 20km downstream from the confluence of rivers Sardon and Tormes. In contrast Sardon river is a seasonal river with peak flow in April-May and November-January.

In the area drained by Sardon River is common to see flooding along several sections of the river in the rainy season, however during the dry months the river does not flow and stagnant water can be found along the river course in the form of pools at the lowest section. (Uria Cornejo, 2000)

## 3. MODEL DESCRIPTION

### 3.1. Model INFIL3.0

The conceptual model of net infiltration forms the basis for development of a daily water-balance model that simulates the processes that affect net infiltration of water across the lower boundary of the root zone (U.S.G.S., 2008). The model consider that In many field applications, net infiltration below the bottom of the root zone can be assumed to equal to recharge to an underlying water-table aquifer.

The daily root-zone water-balance simulation model is based on the governing equation (Eq. 1)

$$NI_d^i = RAIN_d^i + MELT_d^i + Ron_d^i - Roff_d^i - \sum_{j=1}^6 (\Delta W_d^i)_j - ET_d^i \quad \text{Eq. 1}$$

Where  $NI_d^i$  is the net infiltration (for day  $d$  and grid location  $i$ );  $RAIN_d^i$  is precipitation;  $MELT_d^i$  is snowmelt;  $Ron_d^i$  is infiltration to the root zone due to surface-water run-on;  $Roff_d^i$  is surface-water runoff;  $\sum_{j=1}^6 (\Delta W_d^i)_j$  is the total change in root-zone water storage for all six model layers ( $j = 1 - 6$ );  $ET_d^i$  is the total bare-soil evaporation and root-zone transpiration for all six root-zone layers for day  $d$  and grid location  $i$ , (all in millimeters).

For Sardon Catchment, the component of snowmelt was not applied.

### 3.2. Spatial discretization of INFIL3.0

The calculations of INFIL3.0 are based on a three dimensional representation of the drainage basin being simulated. Hence the horizontal and vertical discretization methods have to be properly selected according to the dimensions and characteristics of the catchment.

#### 3.2.1. Horizontal discretization

The model uses square cells of equal size in the horizontal plane, the size of the grid cell have to be specified in meters in the Simulation Control File. A grid of cells consisting of a set of rows and columns is superimposed over the basin of interest with the origin (row 1, column1) positions in the upper right hand corner (Figure 3). The grid serves as the basis to distribute drainage basin characteristics as soil types, hydrogeologic unit, vegetation type, elevation, slope, aspect, terrain variables, and flow routing variables. The version INFIL3.0 allows a maximum of 60,005 grid cells for each simulation.

#### 3.2.2. Vertical discretization

Vertical discretization is defined for each grid cell using one to five soil layers and one underlying bedrock layer (Figure 4). Number and thickness of soil layers depend on the estimated total soil and root zone thickness at each grid cell location (U.S.G.S., 2008). The upper five layers of the model are used to define

root zone characteristics in the soil. The bottom layer can be used to define either (1) root zone characteristics in consolidated bedrock or (2) a sixth soil layer for locations with thick soils.

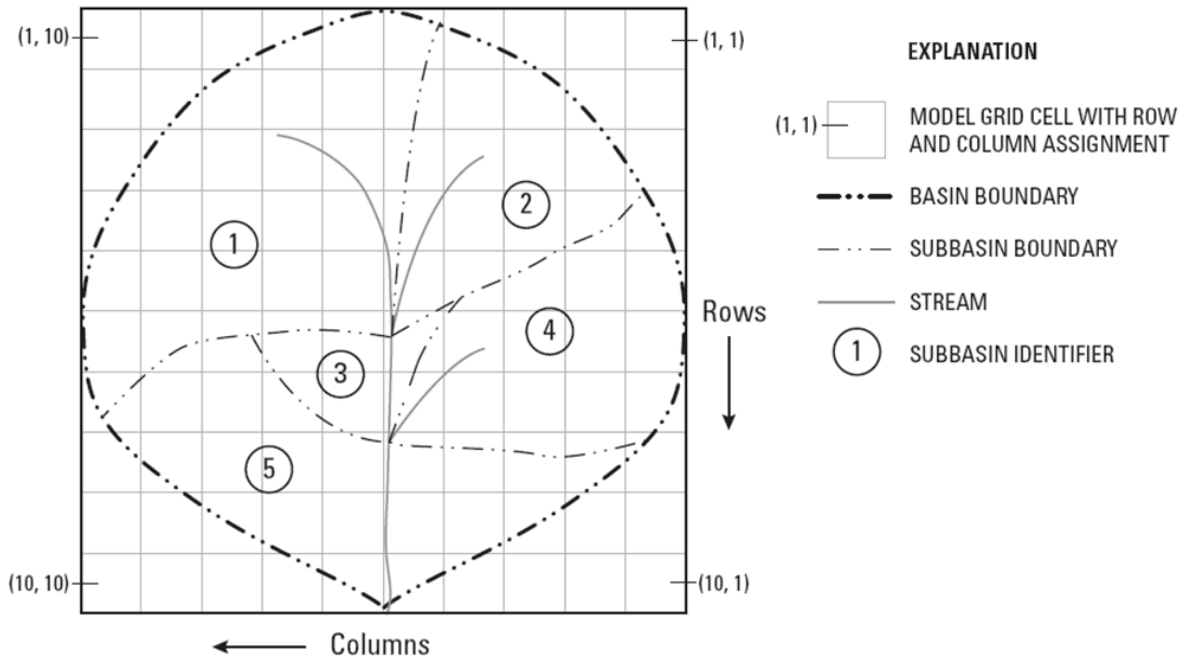


Figure 3. Horizontal discretization of a basin in INFIL3.0 (U.S.G.S., 2008)

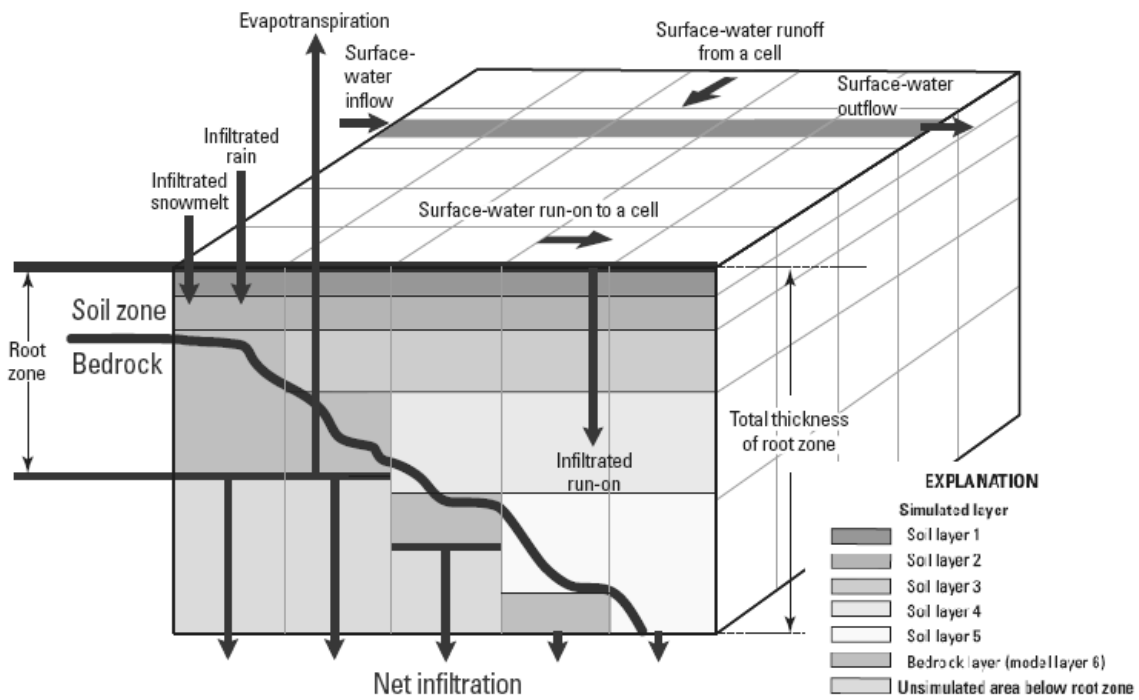


Figure 4. Vertical discretization for INFIL3.0 model (U.S.G.S., 2008).

### 3.3. Spatial distribution of Daily Climate Data

The model distributes daily precipitation and air temperature according two alternative approaches. The first is by using the monthly precipitation/elevation and air temperature/elevation regression models in combination with an inverse distance square interpolation algorithm; and the second is by using a simpler inverse distance squared interpolation model.

### 3.4. Potential Evapotranspiration

Daily evapotranspiration is calculated using a modified form of the Priestley Taylor equation (Eq. 2).

$$\lambda(PET)_d^i = \alpha \left( \frac{S}{S + \gamma} \right)_d^i \left( (Rn)_d^i - G_d^i \right) \quad \text{Eq. 2}$$

Where  $\lambda$  is the latent heat of vaporization of water in mega joules per kilogram;  $(PET)_d^i$  is the rate of potential evapotranspiration at grid location  $i$  at day  $d$  in millimeters per day,  $\alpha$  is the empirical coefficient often set to 1.26 for freely evaporating surfaces.  $S$  is the slope of the saturation vapour pressure temperature curve, in kilopascals per degree Kelvin;  $Rn$  is the incoming radiant energy in mega joules per square meter per day; and.  $G$  is soil heat flux in mega joules per square meter per day.

The term  $\left( \frac{S}{S + \gamma} \right)_d^i$ , which is the slope of the vapour-density deficit curve, is modelled as a function of average daily air temperature by the next equation :

$$\left( \frac{S}{S + \gamma} \right)_d^i = -13.281 + 0.083864(TA_d^i) - 0.00012375(TA_d^i)^2 \quad \text{Eq. 3}$$

Where  $TA_d^i$  is the average daily air temperature on day  $d$  at grid location  $i$  in degrees Kelvin.

The available Energy is  $(Rn)_d^i - G_d^i$ . For INFIL3.0 it is assumed  $G_d^i = 0$  for most cases for a daily time step, meanwhile, total daily net incoming radiant Energy  $(Rn)_d^i$  is equal to the sum of net short wave radiation and net long wave radiation.

#### 3.4.1. Net Incoming radiant Energy

Total daily net incoming radiant Energy  $(Rn)_d^i$  is equal to the difference between net short wave radiation and net long wave radiation. Net long-wave radiation is calculated by the following equation (Eq. 4) from Shuttleworth (1993),

$$Ln = 5.6697 * 10^{-8} (0.98 - \varepsilon_{ac})(TA_d^i)^4 (HSTEP)(3600) \quad \text{Eq. 4}$$

Where  $L_n$  is net long wave radiation in Joules per square meter;  $\mathcal{E}_{ac}$  is clear Sky emissivity, dimensionless;  $TA$  was already defined in Equation 3; HSTEP is the time step in hours, used for calculating total daily evapotranspiration.

The equations used for calculating net short wave radiation are describe in detail by Flint and Childs (1987) and Iqbal (1983) . These equations are applied in the model subroutine POTEVAP to calculate potential evapotranspiration based in atmospheric parameters as well as site geometric properties (latitude and longitude).

**IMPORTANT:** After a review of the equations used in the subroutine POTEVAP it was observed that in the correction factor for standard time at local longitude  $cf$  (Eq. 5) the standard meridian “std” had been fixed to 120 °,

$$cf = (4 * (std - lon(ia) + et) / 60) \quad \text{Eq. 5}$$

Hence, it was necessary to replace the value of the parameter  $std$  according to the location of the study area, otherwise a wrong value of local time and consequently the day duration will produce wrong values of evapotranspiration. This change implied the re-compilation of the source code file because the parameter  $std$  cannot be managed from the input files.

### 3.4.2. Adjusted rate of potential evapotranspiration

The model also takes into account the cloud cover as a variable affecting the energy-balance calculation. The assumption is that the energy for evapotranspiration is reduced in presence of clouds (associated with precipitation); the greater the rainfall, the less the evapotranspiration. For days with precipitation, the modelled clear-sky potential evapotranspiration  $(PET)_d^i$  is reduced by the Equation 6 (U.S.G.S., 2008).

$$(PETRS)_d^i = \frac{(PET)_d^i}{((PETADJ)(PPT)_d^i + 1)} \quad \text{Eq. 6}$$

Where  $(PETRS)_d^i$  is the adjusted rate of potential evapotranspiration at grid location  $i$  and day  $d$  for days with precipitation  $>0$ ;  $(PET)_d^i$  is the (unadjusted) rate of potential evapotranspiration;  $(PETADJ)$  is an empirical adjustment factor to the unadjusted potential evapotranspiration to account for cloud cover and precipitation, a value of 0.16 has been shown to be effective in previous modelling studies (Hevesi, et al., 2003); and  $(PPT)_d^i$  is the rate of precipitation in millimeters per day.

### 3.5. Infiltration, Drainage Evapotranspiration, and Runoff

The INFIL3.0 model uses two subroutines in order to couple surface water flow with the process of infiltration, drainage, and evapotranspiration. The first routine ETINFIL is used to determine infiltration drainage and evapotranspiration from de root zone, while the subroutine SWINFIL calculates the daily runoff generated.

### 3.5.1. Subroutine ETINFIL

This subroutine has four primary steps which are completed for each grid cell for each day (U.S.G.S., 2008).

- (1) *Infiltration and initial calculation of Runoff.*- The infiltration capacity (IC) of the soil and bedrock for each grid cell is calculated on the basis of the saturated hydraulic conductivity of the soil or bedrock. The conductivity value is modified dividing for the duration of summer and winter storms according to the season. The maximum quantity of rain that can infiltrate to the root zone is the value of infiltration capacity previously calculated. Thus, the initial run off is determined as the quantities of rain that are in excess of Infiltration Capacity (U.S.G.S., 2008).
- (2) *Drainage and Redistribution in the Root Zone.*- Infiltration from rain is redistributed downward through the soil layers. First, a calculation is made to verify whether the total water content for the top layer minus the infiltration capacity of the underlying layer is greater than the maximum storage limit for the top layer. The maximum storage limit for the layer is equal to the product of the soil or rock porosity and the thickness of the soil layer (in millimeters). If the total soil-water content for the layer minus the infiltration capacity of the underlying layer is greater than or equal to the maximum storage limit (that is, the layer is saturated), then drainage to the second layer is set equal to the infiltration capacity of the soil. The total soil-water content for layer 1 (top layer) is then updated by subtracting the quantity drained to layer 2. If, however, the total soil-water content for the layer minus the infiltration capacity for the layer is less than the maximum storage limit (that is, the layer is unsaturated), then downward drainage to the second layer is calculated by using a modified form of an empirical drainage model in Jury and others (1991) for approximating water contents and the depth of the wetting front in a draining soil profile (U.S.G.S., 2008).
- (3) *Evapotranspiration from Each Layer of the root zone.*- Evapotranspiration for each layer is calculated by using a modified form of the Priestley-Taylor equation and the updated soil water content calculated by the downward-drainage function for each layer. In the modified equation the empirical coefficient  $\alpha$  is replaced by  $\alpha'$  which relates seasonal changes in soil water content through the next equation

$$\alpha' = \alpha(1 - e^{\beta \cdot \Theta}) \quad \text{Eq. 7}$$

Where  $\alpha$  and  $\beta$  are coefficients and  $\Theta$  is relative saturation. This modified version has been successfully in arid and semiarid environments (de Bruin, 1988; Stannard, 1993).

The modified version of Priestley-Taylor equation is used to calculate both bare soil-evaporation and plant transpiration. Bare soil-evaporation demand is first simulated from the top two model layers. After bare soil evaporation demand has been met, the modified form of the Priestley – Taylor equation is used to simulate plant transpiration from all six model layers. Finally total evapotranspiration within the six model layers will be the sum of the two components of bare soil evaporation and the six model layers transpiration (U.S.G.S., 2008).

- (4) *Final calculations of Net Infiltration, Change in Water Storage in Each Layer of the Root Zone, and Runoff from the Grid Cell.*- Rain drains into layer 6 either directly when a soil is absent, or from the bottom layer of the soil zone. Excess water in the root zone, which contributes to surface water runoff as a saturated-excess or Dunnian-runoff component, is calculated by a redistribution algorithm that

steps sequentially upward through all root-zone layers. To simulate Runoff and the final water content of each of the five soil layers and bedrock layer, the storage capacity of each layer is checked against the quantity of water held in the temporary-storage term for each layer. If the temporary-storage variable exceeds the storage capacity of the layer, the excess water is added to the overlying layer. The algorithm moves sequentially upward through the root-zone layers until all excess water held in temporary storage has been redistributed to overlying layers that have available storage capacity. If excess water remains after the upward redistribution has reached the top soil layer, the excess water is added to the runoff term. The runoff generated by the upward-redistribution process represents the fraction of inflowing water that exceeds the storage capacity of the root zone. Total runoff, for each cell is thus the sum of the excess root-zone water Runoff and the initial runoff calculated as excess rainfall. The last calculation in the subroutine is the change in total water storage of all six layers of the model,

$$\sum_{j=1}^6 (\Delta W_d^i)_j$$

which is equal to the final storage of all six layers ( $j = 1$  through  $6$ ) minus the initial storage at the beginning of the call to the subroutine (U.S.G.S., 2008).

### 3.5.2. Subroutine SWINFIL (Surface-Water Routing)

This subroutine routes daily runoff calculated previously by ETINFIL to downstream cells as surface water run on. During the routing process, run-on can infiltrate back into the root zone and contribute to daily net infiltration. Surface water flow therefore can be coupled to the root zone water balance by the infiltrated run-on component.

SWINFIL uses a simplified form of the ETINFIL downward-drainage algorithm. Water drains into the root zone and underlying layers only when the overlying layer has become fully saturated. Drainage from unsaturated layers, which is simulated in ETINFIL, is not simulated in SWINFIL. The maximum drainage is limited to the saturated hydraulic conductivity of the underlying layer. If the quantity of water in the bottom layer is greater than the saturated hydraulic conductivity of the layer multiplied by the 1-day time step, then net infiltration is equal to the saturated hydraulic conductivity multiplied by the 1-day time step; if, however, the quantity of water in the bottom layer is less than the saturated hydraulic conductivity multiplied by the 1-day time step, then net infiltration is equal to the quantity of water in the bottom layer. The net infiltration from surface-water run-on is defined as run-on net infiltration and is added to the total daily net-infiltration term.

After the net infiltration has been calculated, excess water in the root zone is then calculated using a redistribution algorithm that steps sequentially upward through all root-zone layers, starting at the bottom and moving up to the top layer; this redistribution algorithm is the same as that used in the ETINFIL subroutine. If excess water remains after the upward redistribution has reached the top soil layer, the excess water is added to the downstream-runoff term. The change in total water storage of all six layers of the model  $\Delta W$  which is equal to the final storage of all six layers minus the initial storage at the beginning of the call to SWINFIL, is then updated. Surface-water flow that does not infiltrate into the root zone becomes surface-water discharge from the drainage basin (watershed) being modeled (U.S.G.S., 2008).

## 4. MATERIALS AND METHODS

### 4.1. Data requirements for INFIL3.0 model

Data used for developing INFIL3.0 model can be grouped into three general categories (Figure 5): (1) time series of daily climate data used to drive the water-balance simulation through time; (2) GIS data including raster-based data sources such as the DEM and vector-based digital maps defining vegetation, soils, and geologic units; and (3) time series of stream flow data used for calibration.

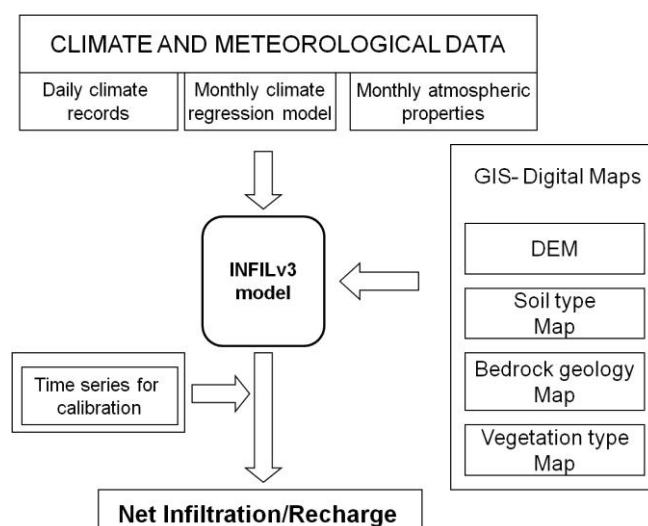


Figure 5. Data Requirements for INFIL3.0 model

### 4.2. Climate data

The Climate data series needed for an INFIL3.0 simulations are: (a) Climate-Stations Information (coordinates and elevation of available stations); (b) Time series of Daily Climate data (precipitation, maximum and minimum air temperatures); (c) Monthly Atmospheric Parameters; (d) Monthly Climate-Regression Models Coefficients. Each of these is showed in the Table 1 with his respective input file name used by INFIL3.0 model in bold text. The methodology used to obtain them is explained in the following subsections

Table 1. Climate Data Requirements for INFIL3.0 model

CLIMATE DATA	Units	Input file name
<b>Climate stations information</b>		<b>sardon.daystations</b>
Coordinates and elevation of available stations		
<b>Time series of daily climate data</b>		
Daily precipitation	[mm]	<b>sardon.precip</b>
Daily Maximum temperature	[°C]	<b>sardon.tmax</b>
Daily Minimum temperature	[°C]	<b>sardon.tmin</b>
<b>Monthly Atmospheric Parameters</b>		<b>sardon.atmos</b>
The ozone-layer thickness	[cm]	
Precipitable water in the atmosphere	[cm]	
Mean atmospheric turbidity	-	

The circumsolar radiation	-	
Surface reflectivity for month. (Albedo)	-	
<b>Monthly Climate-Regression Models Coefficients File</b>		<b>sardon.monthmod</b>
Information about the models used to spatially distribute daily climate variables		

#### 4.2.1. Daily Climate Files

In the Sardon Catchment there are two ADAS (Automated Data Acquisition Systems) installed by ITC. One was installed in the upper catchment (ADAS Muelledes) and the other in the lower catchment (ADAS Trabadillo) Figure 7. According to previous studies (Lubczynski and Gurwin, 2005; Ruwan Rajapakse, 2009) a good correlation exists between the two ADAS stations located in Sardon Catchment, and considering that Trabadillo stations present longer and more continue data series than Muelledes, only Trabadillo ADAS station was selected for representing the precipitation and temperature for the study area.

At the beginning of this study precipitation data series from Trabadillo station were available for the period 24-Sep-2007 to 19-Aug-2010.

In order to fill some gaps presented in Trabadillo ADAS dataset, precipitation data from the Spanish meteorological station Villarmuerto was collected. This station is located 15 km at the Southwest of the catchment (lat: 41°03' 20" N, lon: 6°21'47.2"). The cumulative daily precipitation were plotted to check the correlation between the climatic stations, however an important decrease in the precipitation of Trabadillo station was detected from September 2009 as is shown in Figure 6.

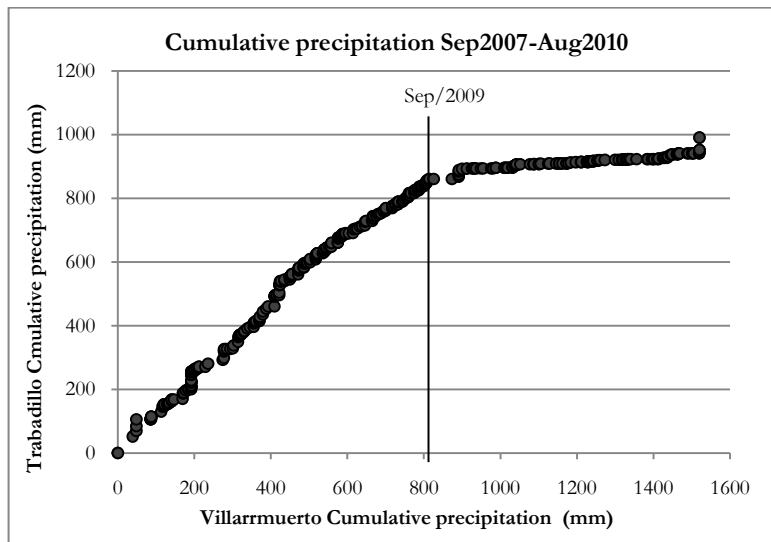


Figure 6. Cumulative precipitations of Trabadillo Station vs. Villarmuerto Station

The precipitation values of Trabadillo after September 2009 are suspiciously low. Due to those lower values detected, it was decided to select a previous period of time for the simulation. The new period selected is the same used by Rajapakse (2009) from 09/2003 to 12/2008

Finally the inputs of Daily Precipitation, Daily maximum and minimum temperature were prepared according to the specifications of INFIL3.0. The three files have the same format and an example can be found in the Appendix A-1.

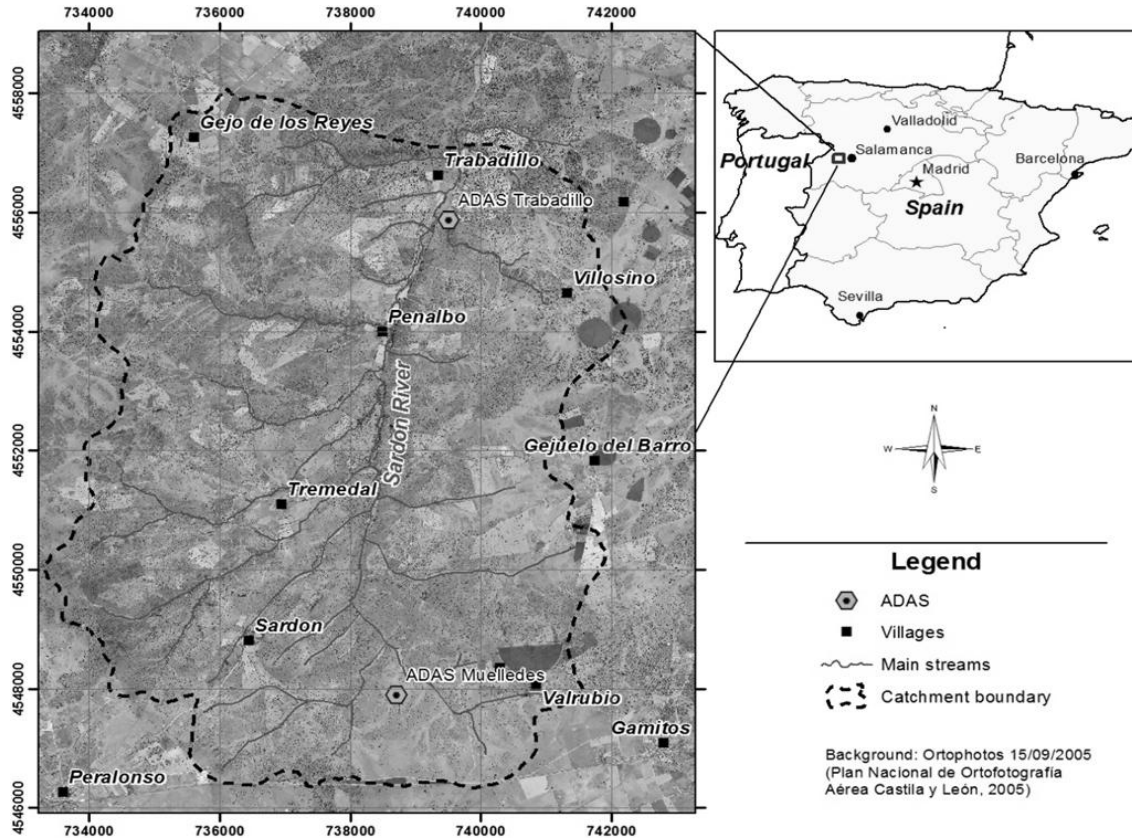


Figure 7. Location of ADAS stations in Sardon Catchment - after (Lubczynski and Gurwin, 2005)

#### 4.2.2. Monthly Climate-Regression Models Coefficients

Because the catchment is not a hilly area the simple inverse distance squared interpolation model was selected to spatially distribute the climate data.

In the Monthly Climate-Regression Model File values for all the coefficients needed for the different methods of distributions of daily climate variables have to be specified, even though only one is used. In the case of choosing the simple inverse distance squared interpolation method, the variables **pptmod**, **tmaxmod**, **tminmod**, need to be set equal to 0 for all the monthly records. A table with the respective parameters used can be found in the Appendix A-2.

#### 4.2.3. Monthly Atmospheric-Parameters File

The monthly atmospheric parameters are used by INFIL3.0 model in order to calculate Net incoming radiant Energy and later, Potential Evapotranspiration. The atmospheric properties are monthly averages of ozone, precipitable water, atmospheric turbidity, circumsolar diffuse radiation, and ground albedo.

The values of ozone layer thickness(considering the day 15th of each month as the representative of the month) were obtained from [http://toms.gsfc.nasa.gov/ozone/ozone\\_v8.html](http://toms.gsfc.nasa.gov/ozone/ozone_v8.html) (NASA, 2011b) according to the respective latitude.

Average monthly values of precipitable water were gotten from AERONET web page <http://aeronet.gsfc.nasa.gov/> (NASA, 2011a).

Atmospheric turbidity values were obtained adjusting values of monthly Aerosol optical depth from AERONET with an Angstrom parameter value of 1.3 according to Iqbal (1983).

In the case of circumsolar radiation according with Flint and Childs (1987) a value of 0.5 can be assumed as a constant value.

The surface reflectivity values were obtained from the Eddy Tower that belongs to ITC and is located in Trabadillo. In this case there were hourly data available for the 9 first months of 2010, the albedo was calculated and averaged for these months meanwhile for the rest of month an average was assumed.

The input Monthly Atmospheric-Parameter File is showed in the Table 4.

### 4.3. GIS data

The primary GIS data sources needed for the development of an INFIL3.0 model are the DEM, Soil units map, Geologic units map, and Vegetation map. Each of them with their specific parameters needed and the method of acquisition or respective source are shown in Table 2.

Table 2. GIS Data Requirements for INFIL3.0 model

GIS DATA	Units	Method of Acquisition/Source	Input file Name INFIL3.0
<b>DEM</b>		National Plan of Aerial Ortophotogrametry, Spain	<b>sardon.gwc</b>
	[m]	DEM 5m resolution	
<b>Soils Map</b>		Based on Geomorphologic Map IGME	<b>sardon.soils</b>
Field capacity,	-	Field measurements and Laboratory analysis	
wilting point water content,	-		
porosity,	-		
Soil drainage function coefficient (Beta)	-	Based on (Campbell, 1985)	
saturated vertical hydraulic conductivity, and	[mm/d]	Field measurements and Laboratory analysis	
total soil thickness	[m]	GIS method	
<b>Bedrock Map</b>		(Tsfai, 2000)	<b>sardon.bedrock</b>
The effective root zone porosity for the bedrock layer,			
Saturated vertical hydraulic conductivity.	[mm/d]	(Shakya, 2001)	
<b>Vegetation Map</b>		Vegetation Map Sardon Catchment (Reyes and Lubczynski, 2011)	<b>sardon.veget</b>
Percentage of root density for each of the six layers of the model.	%	Literature review: (Canadell, et al., 1996; Hernández, et al., 2008; López, et al., 2001; Silva, et al., 2003)	
The root-zone depths from land surface, (ly1-5)	[m]	Literature review: (Canadell, et al., 1996; Hernández, et al., 2008; López, et al., 2001)	

#### 4.4. Digital Elevation Model - DEM

The Digital Elevation Model (DEM) is one of the most important inputs because based on it the horizontal discretization will be done. The source of the DEM was the National Plan of Aerial Orthophotogrametry of Spain and its spatial resolution is 5 m. However INFIL3.0 has a restriction for the number of grid cells allowed in each simulation. In total information for 60,005 grid cells (pixels) can be specified for each simulation in INFIL3.0. Therefore the final grid size must be in accordance not only with the grid cell restrictions, but also with the scale and spatial resolutions of every input map to be used in the simulation.

##### 4.4.1. Grid cell size analysis

Since the model has not a handy interface to manage several sub catchments easily, in order to optimize the time of simulation and the computer processing power, it was decided to handle the entire catchment as only one unit. The grid cell size for this catchment has to be suitable for the properties of the input data and at the same time it should satisfy the condition of maximum number of pixels allowed.

So first of all and according to the methodology explained in Hengl (2006) the recommended grid cell size for each of the inputs map was calculated (Table 3). Then the minimum pixel size for the catchment was calculated dividing the total area of the catchment (75.8 km<sup>2</sup>) by the maximum number of pixels allowed in each simulation (60,005).

The result of this last operation was a minimum area equal to 1,264m<sup>2</sup>; it means a grid cell side of 35.5 m. In order to not work in the limit but also with a close value, it was rounded at 40m.

Table 3. Grid cell size for the input maps

Input Map	Scale factor SN	Recommended grid size (m):		
		Coarsest	Finest	Best
Geologic Map	50,000	125	5	25
Geomorphology Map	50,000	125	5	25
		Spatial resolution		
Vegetation Map		1 m		
DEM		5m		

Forty meters is proper within the limits of the recommended grid sizes showed in the Table 3. Hence this value will be adopted for the simulations of the present study.

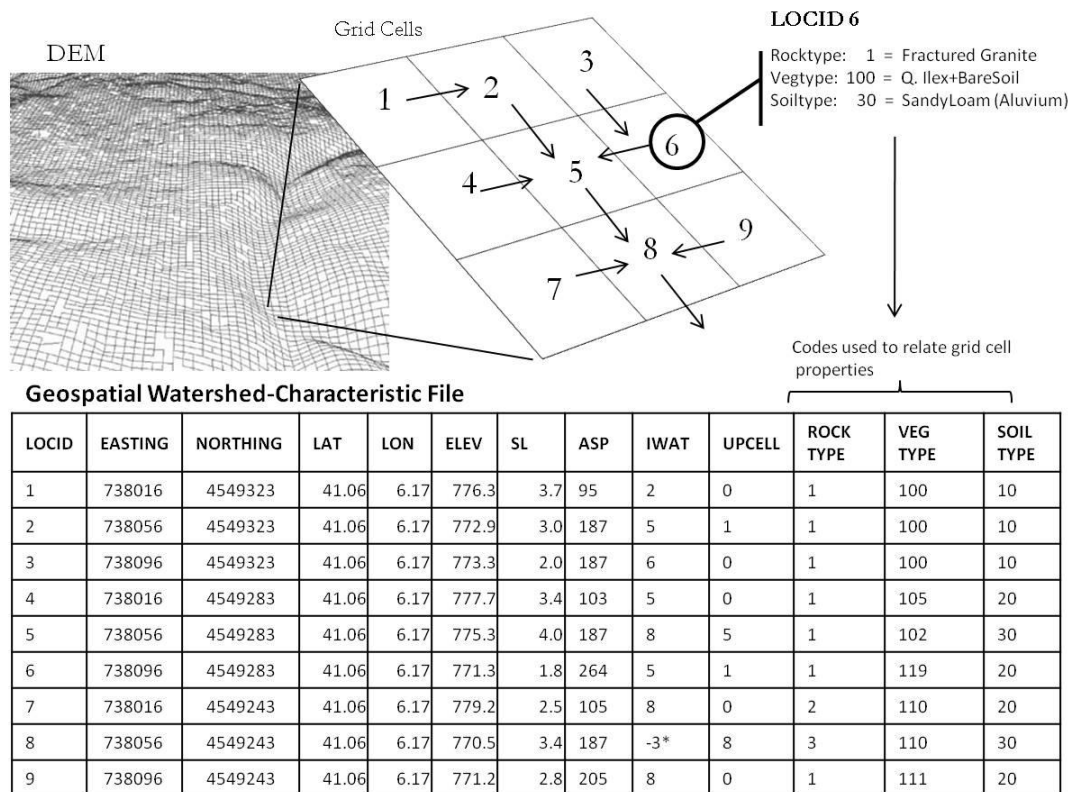
##### 4.4.2. Geospatial Watershed-Characteristic File

The Geospatial Watershed-Characteristic File (**Sardon.gwc**) is used by INFIL3.0 to distribute spatially the characteristics of the watershed for each grid cell of the model. In this study an array of 47404 cells of 40m per side was created over the catchment area and was codified according to INFIL requirements.

Products derived from the DEM as SLOPE and ASPECT maps processed with GIS functions were used to give characteristic to each grid cell of the model. The software used was ArcGIS10 with the extensions 3D Analyst and ArcHydro (Maidment, 2002). The main variables for the Geospatial watershed-characteristic file are mentioned below with the respective INFIL variable name in bold text:

- Coordinates of the centroid of the grid cell easting, northing, latitude, longitude and elevation, that are stored in the INFIL variables (**easting, nothing, lat, lon, elev**).
- Row and column indicator that define the position of the grid cell (**row, col**), see Figure 3.
- The land surface slope of the centroid of the grid cell (**sl**) in degrees, the land surface aspect of the centroid of the grid cell, degrees azimuth relative to the north (**asp**).
- Variable **locid** which is a sequential number of the grid cell in the upstream to downstream ordering.
- Variable **iwat** is the locid identifier of downstream cell to which run off is directed from the current cell. This was calculated by using the flow direction algorithm of ArcHydro (Maidment, 2002) and combining with overlapping function in ArcGIS10.
- Variable **upcell** is the total number of cells upstream to the current grid cell, this value was calculated using flow accumulation algorithm of ArcHydro extension.
- The variables fraction of viewable sky **skyview** was set equal to 0.9 and blocking ridge angles **ridge(36)** set equal to 1, because of the prevailing flat landscape in the study area.
- The variables **rocktype**, **vegtype** and **soiltype** are codes that join the watershed file to the respective properties files described in the following sections.

The following Figure 8, shows an example of how the main variables of Geospatial Watershed-Characteristic File are defined



\* A value of iwat = -3 identifies the out flow of the basin

Figure 8. Example of Geospatial Watershed Characteristic File Variables.

#### 4.5. Soil Map

The methodology adapted to do the Soil Map consists of combining the Geomorphologic Units with Geomorphometry properties extracted from the DEM, to classify the catchment area into similar zones. After that every zone was characterized by the soil properties from the samples collected in fieldwork.

The Geomorphologic Map (IGME, 1991a, 1991b) was also used as reference to take soil samples and to do infiltration tests over their geomorphologic units.

Hydraulic properties needed for INFIL3.0 as inputs consisted of: soil saturated vertical hydraulic conductivity, soil porosity, soil field capacity, wilting point and the soil drainage-function coefficient

##### 4.5.1. Field data and Laboratory Analysis

A total of 49 soil samples were collected at 10 locations over different geomorphologic units and in different depths with the purpose of derive their soil hydraulic parameters by laboratory analysis.

Samples were collected in two ways; one was ring sampler (undisturbed sample) and another in sample bags. A summary of the soil samples with their coordinates is showed in the Appendix B-1. In total 16 ring samples and 33 bags were collected during the fieldwork campaign, their distribution in the catchment is showed in Figure 9. The samples collected in bags were used in the textural analysis meanwhile the rings samples were tested in the permeameter.

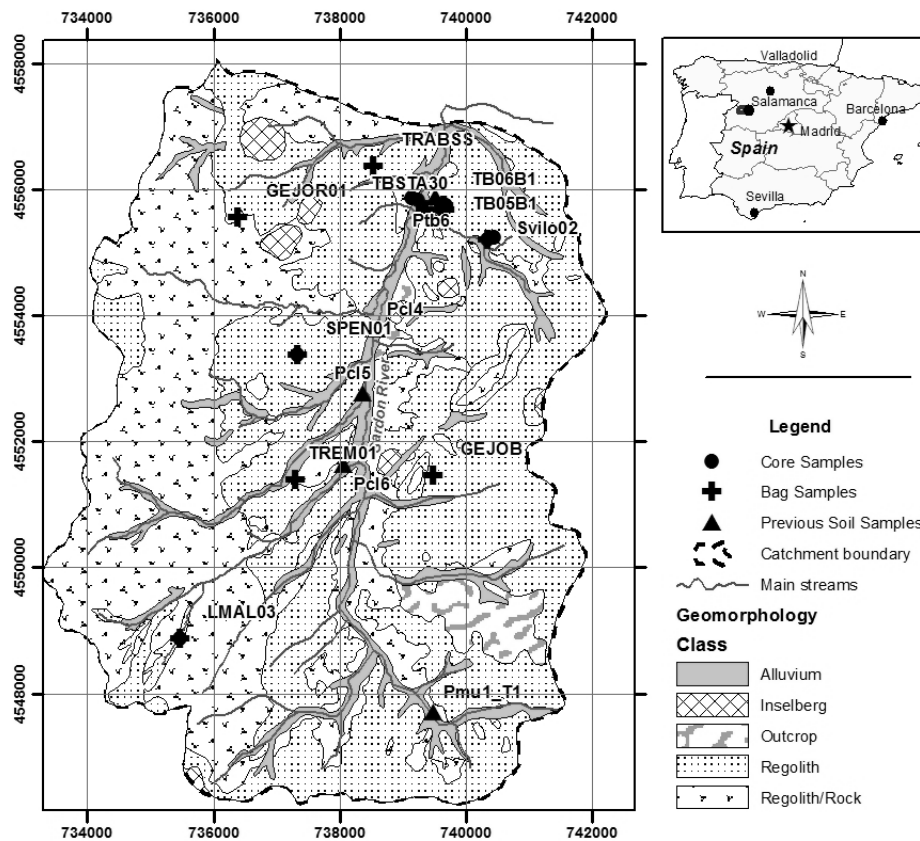


Figure 9. Soil samples locations

The textural analysis of the collected soil bag samples was done in the laboratory with the pipette method to determine the particle size distribution (quantity of sand, silt, and clay fractions in samples of soil). First the soil sample was sieved to separate the gravel (particles coarser than 2mm) from grains less than 2mm in diameter and the percent of sand was isolated by sieving through a set of nested sieves. The silts and clays in each sample were determined by using a pipette method that measures the actual percent by weight of each particle size class in the sample. The details of the particle size distribution analysis using the pipette method can be found in the laboratory manual Procedures for Soil Analysis (van Reeuwijk, 2002).

Besides, to improve the number of soil samples in the area, data collected in Berhe (2010) were used. The location of these points is also shown in the Figure 9.

The laboratory analysis of soil samples used to derive the soil hydraulic parameters is separately discussed below.

#### 4.5.2. Soil and Water characteristics Software

The software Soil and Water Characteristics that is part of SPAW (Soil-Plant-Air-Water), model developed by USDA Agricultural Research Service, which can present soil hydraulic parameters from the provided percent of sand, silt and clay. The percent of sand, silt and clay of the soil samples analyzed in the lab through the pipette method was used to derive soil hydraulic properties using SPAW. The main hydraulic parameters of interest for INFIL3.0 are field capacity, wilting point, saturated hydraulic conductivity, porosity.

#### 4.5.3. Soil drainage-function coefficient

There is an extra variable essential for INFIL3.0 that is soil drainage function coefficient (**soilb**), this can be derived also from the textural analysis and applying the following equations found in Campbell (1985):

$$b = -2\psi_{es} + 0.2\sigma_g \quad \text{Eq. 8}$$

Where  $\psi_{es}$  is the air entry potential at standard bulk density of  $1.3 \text{ Mg m}^{-3}$  and can be calculated with the Equation 9, and  $\sigma_g$  is the geometric standard deviation of the particles derived from the Equations 10 to 12.

$$\psi_{es} = -0.5d_g^{-1/2} \quad \text{Eq. 9}$$

$$\sigma_g = e^s \quad \text{Eq. 10}$$

$$d_g = e^a \quad \text{Eq. 11}$$

Where  $d_g$  is mean particle diameter, and the values of  $a$  and  $s$  are calculated with the equations Eq. 12 and Eq.13.

$$a = \sum m_i \ln(d_i) \quad \text{Eq. 12}$$

$$s = \left[ \sum m_i \ln(d_i)^2 - a^2 \right]^{1/2} \quad \text{Eq. 13}$$

In the preceding equations  $m_i$  is the mass fraction of textural class  $i$ , and  $d_i$  is the arithmetic mean diameter of class  $i$ . The summation is taken over the three textural classes, sand, silt and clay. For the three classes normally used in determining texture,  $d_{\text{clay}} = 0.001\text{mm}$ ,  $d_{\text{silt}} = 0.026\text{mm}$ ,  $d_{\text{sand}} = 1.025\text{mm}$ .

#### 4.5.4. Permeameter

The 16 undisturbed soil samples for saturated hydraulic conductivity were taken in metallic rings of 53 cm diameter and 100 cm<sup>3</sup> volumes with a closed ring holder. The Permeameter (Eijkelkamp) used in laboratory allows two methods to determine the permeability: measuring with constant water head and with falling water head. The selection of the method depend if the samples are highly, moderately or poorly permeable.

The constant head method is used for non-cohesive, high permeability sediments such as gravels or sands, and the falling head method is more suitable for cohesive, intermediate to low permeability sediments such as loams or structured clays. For more details of Permeameter laboratory operations see the Operating instructions at Eijkelkamp Webpage (2010).

#### 4.5.5. Double Ring Infiltration Test

Infiltration rates were measured with the standard double-ring infiltrometer (FAO, 1974) in 11 locations of the catchment see Figure 13. A list with coordinates of locations is shown in Appendix B-2. At each location two to six repetitions were done and a total were 24 infiltration tests. The infiltration capacity derived from the infiltration rate was plotted against the cumulative time and fitted with a power function line through the points. The receding line showing a constant value was used to read the saturated hydraulic conductivity value.

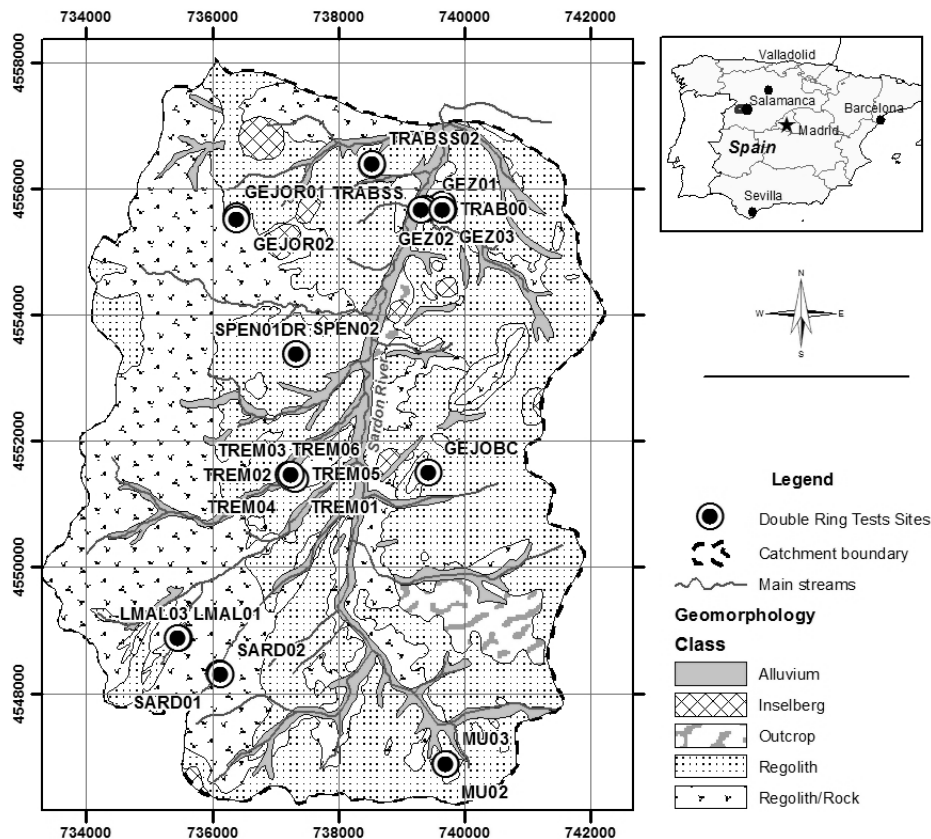


Figure 10. Locations of infiltration tests.

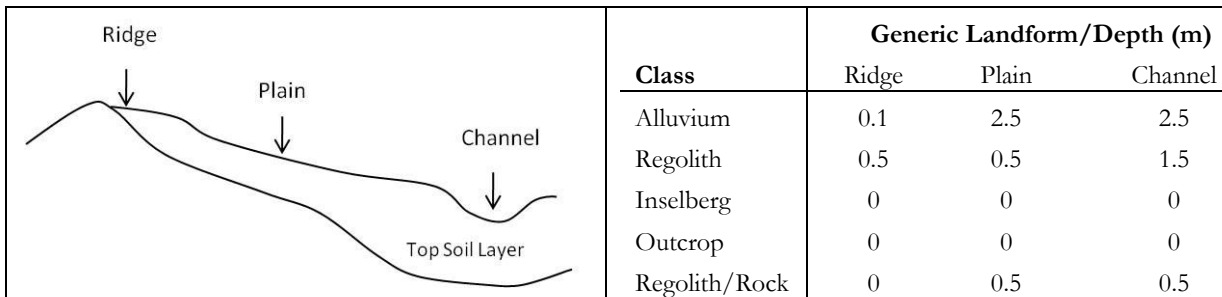
#### 4.5.6. Soil Depth Map

The Soil depth map was derived using measurements of depths collected during fieldwork, in combination with the high resolution DEM available for the catchment and with the Geomorphologic Map (IGME, 1991a, 1991b). Because of the relief is one of the most important factors of soil formations, has been demonstrated that DEM is a useful secondary information source for the prediction of soil properties (Grunwald, 2006), and many case studies has been developed (Dobos and Hengl, 2009; Gobin, et al., 2001; McBratney, et al., 2000).

First, geomorphological homogeneous areas were established in order to correlate them with the field measurements of soil depth. Geomorphological homogeneous landform classes were defined using the Geomorphologic Map in combination with a Generic landforms map. The methodology to get the Generic landforms map is explained in Hengl and Reuter (2009). It basically consists on shape algorithms based on DEM parameterization, slope, aspect and geoforms relationships. After this process, land features like ridge, plain and channels are identified anywhere in the DEM.

Once these values of depth are distributed over different homogeneous areas, they were interpolated using the Ordinary Kriging algorithm. The Flow chart of this process is showed in Figure 12.

The different generic landforms were associated to values obtained during the fieldwork as is shown in the Figure 11:



Class	Generic Landform/Depth (m)		
	Ridge	Plain	Channel
Alluvium	0.1	2.5	2.5
Regolith	0.5	0.5	1.5
Inselberg	0	0	0
Outcrop	0	0	0
Regolith/Rock	0	0.5	0.5

Figure 11. Generic landforms associated to soil depth

#### 4.5.7. Soil Class Map

The Soil class Map was done using a similar process to the Soil depth map, but in this case the soil hydraulic properties obtained from the lab analysis were used to characterize the Geomorphologic units.

In several locations where the samples were taken at different depths, a weighted average was applied to calculate a representative value. Then values of saturated conductivity established in fieldwork experiments were compared with those obtained from laboratory.

The last step was to create the corresponding Soil characteristic file **Sardon.soils** according to the INIFL3.0 specifications.

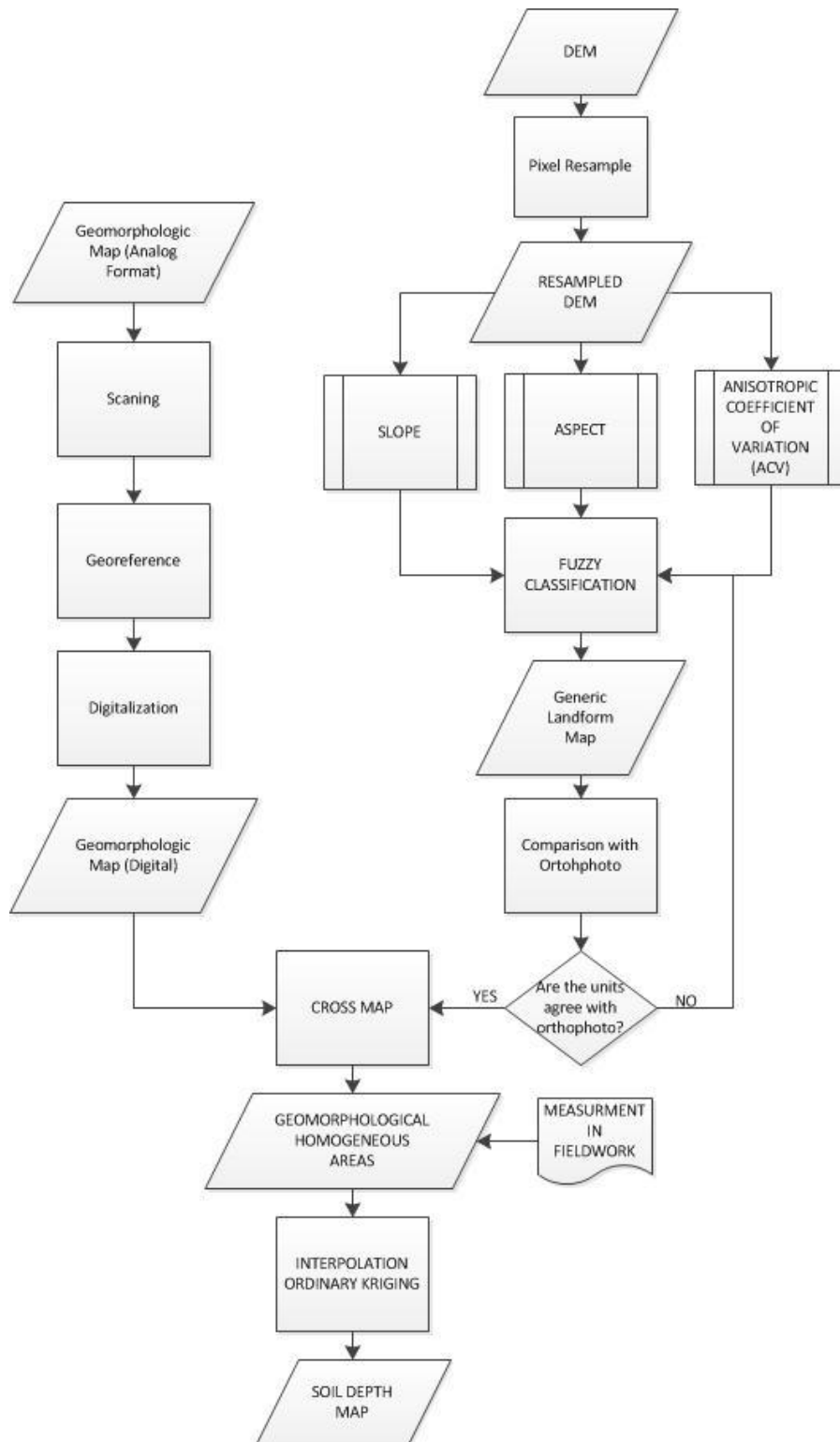


Figure 12. Soil depth map flowchart

#### 4.6. Bedrock Map

The bedrock map was compiled from Tesfai (2000), and the units were reclassified and assigned according to the format needed by INFIL3.0. The values of saturated hydraulic conductivity and porosity needed to create the input bedrock file were obtained from the literature review.

A look at the existing literature on the area indicates hydraulic conductivity is a highly variable aquifer parameter, depending on the weathering and fracturing intensity of the local environment. Uria Cornejo (2000) cited values between 0.01 to over 100m/day according to Kagaba(1997), and between 0.05 to 91.7 m/day according to Duah (1999).

Furthermore, according to Shakya (2001) shallow groundwater is commonly stored in the weathered layer with porosity between 5-30%, the same author has used an average effective porosity of 1% as representative of the study area.

Then, the properties assigned to bedrock map were assigned to represent a low vertical hydraulic conductivity in the massive granite equal to 0.001mm/day with a porosity of 1%; for the fractured granite vertical hydraulic conductivity equal to 0.1 mm/day with a porosity of 10%, and, for the unconsolidated rocks a vertical hydraulic conductivity of 1mm/day with porosity equal to 30%.

#### 4.7. Vegetation Map

In INFIL3.0 model is necessary to assign a class vegetation code for each grid cell in the watershed file (**Sardon.gwc**), and then to create the corresponding vegetation file (**Sardon.veget**) that contains the variables to be used for each class. There are three important variables that define a vegetation class, those are: vegetation cover (**vegcover0**: percentage of land surface covered by vegetation), percentage of root density (**vegcover(6)**), and root zone depths (**rzdpth(6)**) for each layer to be modelled.

The source of the vegetation map was the image classification done by Reyes (2011) for the Sardon area. The image used in that procedure was a Quick Bird Image with spatial resolution of 0.60m. This classification show the most important vegetation classes in the study area *Q. Ilex* and *Q. Pyrenaica* according to Lubczynski and Gurwin (2005) .

##### 4.7.1. Segmentation of classes for Vegetation map

The model allows only one class of vegetation per grid cell, represented by a code, this class is defined by the percentage of land surface covered by vegetation in the grid area, the complementary percentage will be assumed, by the model, as bare soil. This fact was controlled by creating mixture classes and modifying the parameters that control bare soil behaviour.

In the classified map from Reyes (2011) it is possible identify the two main species of oak trees (*Q. Ilex*, & *Q. Pyrenaica* ) present in the area, and a third one was assumed as a mixture among bare soil, grass, and shrub. Thus, in each pixel it is possible to have big number of combinations of vegetation coverage types (Figure 13). So the solution choice was to create discrete classes, and then assign to each pixel the closest one.

The discrete classes were created combining values of percentages multiples of 5% for each class, (for instance: a class containing: 5% of *Q. Ilex*, 5% of *Q. Pyrenaica*, and 90% of bare soil; or 10% of *Q. Ilex*, 25% of *Q. Pyrenaica*, and 65% of bare soil). The value of 5 % was chosen because is mathematically handy, and in turn keeps the high-resolution of the vegetation coverage map. As well the total number of combinations created is feasible compared with the 500 classes allowed by INFIL3.0 model.

A total of 231 classes were established, but still taking in account the three coverages (*Q. Ilex*, *Q. Pyrenaica*, and bare soil), to manage this issue, the oaks species were grouped in one adding its respective percentages, and weighting their properties values (root density and maximum root depth) according to its relative percentage. For instance a class containing: 5% of *Q. Ilex*, 15% of *Q. Pyrenaica*, and 80% of bare soil was converted into a new one with a mixed class of 20% *Q. Ilex-Q. Pyrenaica* and 80% of bare soil. So the respective properties will be weighted with a weight factor of 5/20 for *Q. Ilex*, and 15/20 for *Q. Pyrenaica*.

Once the empirical classes had been created, the next step was to assign the respective code for each grid cell according to its coverage percents; first it was necessary to know what type and the percentage of vegetation cover are inside of every grid cell in the study area and then match it with the closest created class.

The procedure was possible since the classified image has higher resolution (0.60 m) compared with the grid cell size used to represent the catchment (40x40m). Using ArcGIS10 software, the Intersect operation was applied between the net representing the grid cells in the catchment and the vegetation cover, so every pixel got its individual percentages. One sample pixel is showed in the following Figure 13.

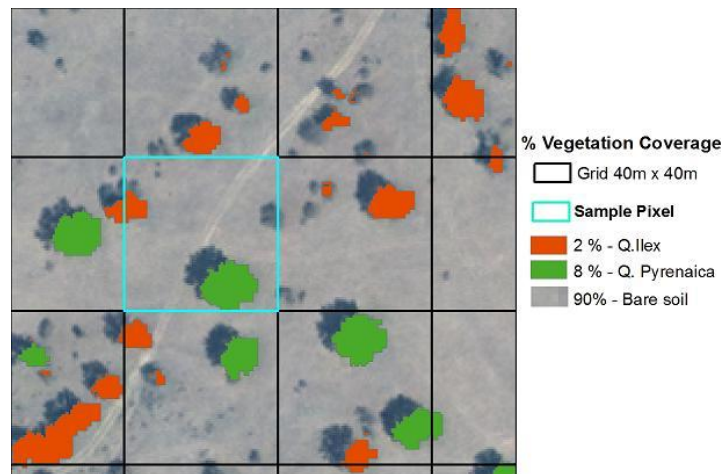


Figure 13. Sample pixel with its percentage of vegetation classes

After percentages of vegetation for every grid cell has been calculated, it was necessary to round them into the closest value multiple of five. Promptly each pixel is matched with one of the 231 classes previously created. The details of this step can be found in the Appendix C-1.

#### 4.7.2. Vertical discretization

INFIL3.0 allows the vertical discretization according to the vegetation cover attributed for each cell grid. In this study the discretization was done according to soil matric potential profiles installed near of Trabadillo ADAS station. This discretization allowed the comparison of the soil water content values derived from the measurements with the results from the simulations.

Vertical discretization is determined also by the maximum root depth of the vegetation cover. These values were obtained from the literature; for the case *Q. Ilex* according to Canadell, et al. (1996) a maximum depth of 3.7m was set, and for *Q. Pyrenaica* a maximum root depth equal to 6m according to

Silva, et al. (2003). The following figure shown the values of vertical discretization assumed for the modelling.

	Depth	Thickness	Root Density Q. Ilex	Root Density Q. Pyrenaica	Water Mark sensors
Layer 1	0.38m	0.38m	90	90	--- 0.25---
Layer 2	0.63m	0.25m	90	90	--- 0.50---
Layer 3	0.88m	0.25m	50	70	--- 0.75---
Layer 4	1.13m	0.25m	30	30	--- 1.00---
Layer 5	Q. Ilex: 3m Q. Pyrenaica: 5m		20	20	
Layer 6	Q. . Ilex: Maximum Root depth= 3.7m*  Q. Pyrenaica: Maximum Root depth= 6m		10	10	

Figure 14. Vertical discretization for the species *Q. Ilex* & *Q. Pyrenaica*

The percentages of root density attributable to the species *Q. Ilex* and *Q. Pyrenaica* are variables not well defined in the documentation of the model. It is only indicated that express its decreasing according to the depth. However from root densities studies (Hernández, et al., 2008; López, et al., 2001) it was estimated that the root density is higher in the first layers and continue decreasing until reach a minimum 10% in the lowest layer.

#### 4.7.3. Adjustment of Bare Soil Parameters

As mentioned above INFIL3.0 computes separately the percentage of bare soil coverage present in a cell grid, but in the case of the Sardon catchment bare soil usually is mixed with grass. This effect has to be considered in the variables that control bare soil evaporation.

The estimation of soil transpiration in INFIL is given by the formula

$$BSE = \alpha' * PET \quad \text{Eq. 14}$$

Where  $\alpha'$  (see also, Chapter 3, Eq. 7) is working as crop coefficient (Kc), so adopted solution was to find the parameters  $\alpha$  and  $\beta$  that adjust the equation for a Kc of grass.

$$\alpha' = \alpha (1 - e^{-\beta \theta})$$

Therefore, finding such values it was possible to fit an intermediate curve that represents the mixture of grass and bare soil evapotranspiration.

To achieve the mentioned purpose the TAW (Total available water) for grass was calculated according to FAO 56 (Allen and FAO, 1998), Eq. 15

$$TAW_{grass} = 1000(\theta_{FC} - \theta_{WP})Zr \quad \text{Eq. 15}$$

Where  $\theta_{FC}$  is the water content at field capacity [ $\text{m}^3 \text{m}^{-3}$ ];  $\theta_{WP}$  is the water content at wilting point [ $\text{m}^3 \text{m}^{-3}$ ] and  $Zr$  the root zone depth [m].

The values of field capacity were considered from the average of the soil samples and the same for the wilting point values. The root zone depth assumes the values of grazing pasture according to FAO 56 with a depletion factor of 0.6 (FAO56- Table 22).

Replacing in Eq. 15, we have:  $TAW_{grass} = 1000(0.15 - 0.06) * 0.5 = 45\text{mm}$

After calculating  $TAW$ , the readily available water  $RAW$  can be calculated applying the following equation

$$RAW_{grass} = p * TAW_{grass} \quad \text{Eq. 16}$$

Where  $p$  is the average fraction of Total Available Soil Water that can be depleted from the root zone before moisture stress. This was taken as 0.6 for Grazing pasture, and the result is  $RAW_{grass} = 0.6 * 45 = 27$

Then these values were plotted with the aim to calculate  $K_s$  water stress coefficient  $\theta_t$  Figure 15

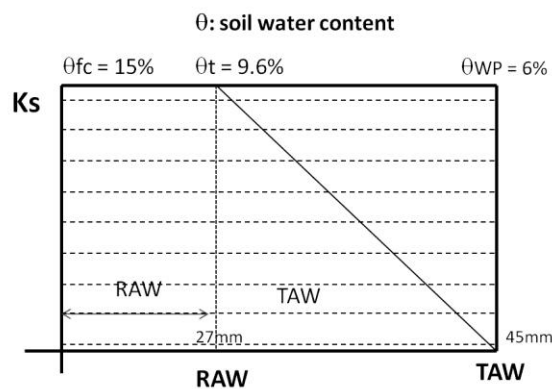


Figure 15. Water stress coefficient,  $K_s$

Then with  $\theta_t = 9.6\%$ , relative saturation  $\Theta$  was calculated applying the following equation (Eq. 17), the result was  $\Theta = 0.1$ :

$$\Theta = (\theta - \theta_{WP}) / (\theta_{sat} - \theta_{WP}) \quad \text{Eq. 17}$$

The curve  $Kc = \alpha(1 - e^{\beta\Theta})$  was plotted as shown in the Figure 16, with the parameters  $\alpha = 1.04$  and  $\beta = -10$  for bare soil and with value of  $Kc$  for grass. After that an average curve was fitted which represent a mixture of bare soil and grass. The new parameters for this new curve were

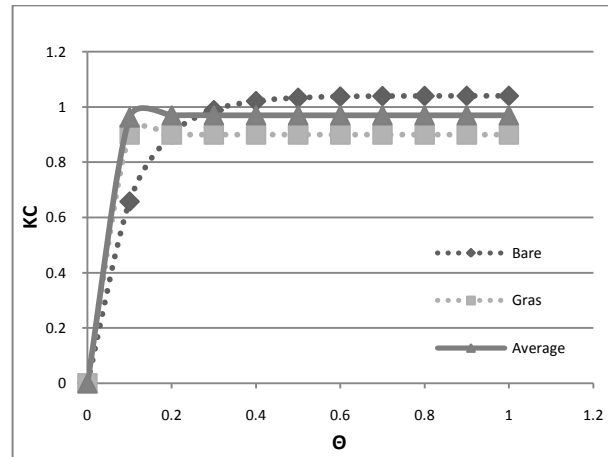


Figure 16. Curves of adjusted parameters  $\alpha, \beta$

#### 4.8. Model Set up and Initial conditions

The simulation control file must be prepared for each INFIL3.0 simulation. It contains the model input variables including the simulation time period and the names of data-input and model-output files.

The most important input and output files that have to be specified in the control file are listed in the Appendix D-1, more details about the variables can be found in the Documentation of Computer Program INFIL3.0 (U.S.G.S., 2008).

#### 4.9. Evaluation of the Model

In order to evaluate the results of the model some comparison were done. First the simulated potential evapotranspiration calculated by the model with the modified Priestley Taylor equation (de Bruin, 1988) were compared with information at Trabadillo's Eddy Tower, and also values of soil moisture derived from water mark sensors installed close to Trabadillo ADAS station were compared with values of soil water content simulated over the cell grid that correspond to the closest position of the Trabadillo station.

## 5. RESULTS AND DISCUSSION

### 5.1. Data Acquisition

#### 5.1.1. Climate data

INFIL3.0 model requires three years of warming up period. Therefore time series of climate data from September 2003 to December 2008 were selected to develop the model. The first three years from September 2003 to December 2006 were used as warming up period and the simulations were considered for the following period from January 2007 to December 2008.

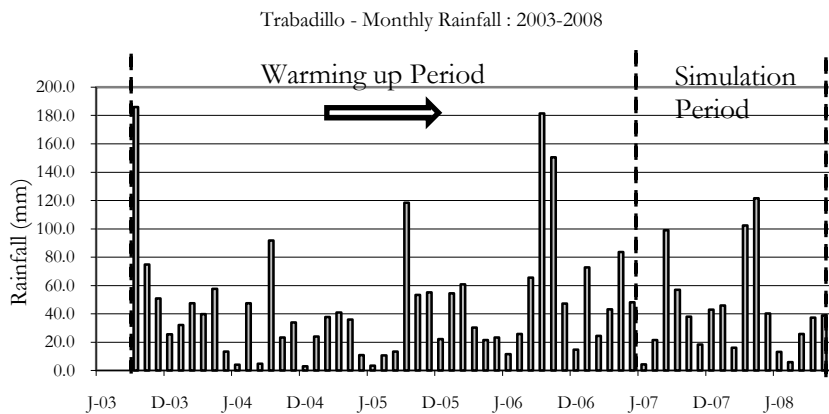


Figure 17. Monthly Rainfall in Trabadillo station showing warming up and simulation periods.

The period of simulation could not be extended due to the reasons explained in the section 4.2.1.

#### 5.1.2. Monthly atmospheric parameters

The monthly atmospheric parameters found in this study are shown in Table 4. Those parameters are controlling the driving force potential evapotranspiration calculated in INFIL3.0 by modified Priestley Taylor equation (de Bruin, 1988).

Table 4. Monthly Atmospheric Parameters

	Ozone (cm)	Precipitable water (cm)	Atmospheric turbidity	Fraction of circumsolar radiation	Surface reflectivity
Month	ozone	wp	Beta	csr	pg
January	0.29	0.87	0.061	0.5	0.22
February	0.29	1.01	0.044	0.5	0.20
March	0.33	0.84	0.042	0.5	0.21
April	0.41	1.40	0.078	0.5	0.22
May	0.36	1.40	0.048	0.5	0.22
June	0.33	1.50	0.050	0.5	0.22
July	0.29	1.60	0.040	0.5	0.23
August	0.33	1.72	0.040	0.5	0.24

	Ozone (cm)	Precipitable water (cm)	Atmospheric turbidity	Fraction of circumsolar radiation	Surface reflectivity
September	0.31	1.82	0.093	0.5	0.21
October	0.26	1.51	0.040	0.5	0.22
November	0.30	0.92	0.022	0.5	0.22
December	0.25	0.95	0.022	0.5	0.22

Figure 18 shown Potential evapotranspiration calculated for Trabadillo station. The rank of values are between a 0.5 mm/d. and a of 6.3 mm/d. These values are in similar to those calculated by Uria Cornejo (2000) (0.5 6.5mm/d) in the period 1998-1999 and by Berhe (2010) (0.4-7mm/d.) in the period June 2008 to September 2009, both calculated with Penman Monteith equation.

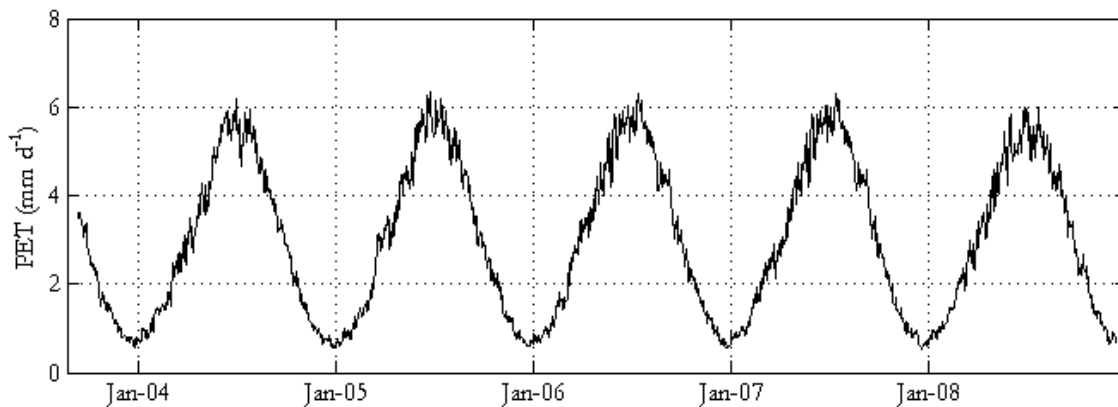


Figure 18. Potential evapotranspiration calculated with modified Priestley-Taylor equation by INFIL3.0 model

### 5.1.3. Soil Textural Analysis

Soil samples were taken from 10 locations, in 7 of those locations sampling was at different depths making a soil profile, there were a total of 33 samples processed in the Lab with the pipette method. Most of the samples soil textural class was established as Sandy-Loam . A list with the results is in the Appendix B-3.

In the analysis of profile samples was found that the percentage of sand increases as the sample is deeper, and proportionally decrease the percentage of silt. This fact can be appreciated in the following Figure 19 and Figure 20, at different depths. Two points, one near to Trabadillo station (TBSTA30) and the second close to Tremedal Village (TREMSS)(the decreasing in colour intensity from represents gradient of depth.)



Table 5. Summary of Soil Hydraulic properties derived from different laboratory and field methods.

N.	Sample ID	Description	Saturated Hydraulic conductivity Ksat (mm/d)			Field Capacity (%vol)		Wilting Point (%vol)	Porosity (%vol)		Beta -
			SPAW	Perm*	DR*	SPAW	Perm	SPAW	SPAW	Perm	(Campbell, 1985)
1	LMAL03	Los Malones	1406	143	1524	15.2	26.2	5.9	44.1	32.7	3.3
2	TB05B1	Trabadillo La Mata	1603		4320	13.8		4.7	44.5		2.6
3	TB06B1	La Mata	772		576	19.5		9.9	43.1		4.9
4	TREMSS	Tremedal A	1951		924	12.8		4.4	44.8		2.8
5	GEJOR	Gejo de los Reyes	1246		4361	16.3		6.7	44.0		3.7
6	TRABSS	Albarranes	806		1740	19.8		8.4	43.8		4.5
7	TBSTA	Trabadillo station	1320			15.7		4.9	44.5		2.7
8	GEJOB	Gejuelo del Barro	1432		3200	13.9		5.0	44.4		2.7
9	SVILL2	Via Villosino	797	1317		18.5	28.1	7.3	43.9	32.3	3.8
10	SPEN1	Penalbo	724	542	1440	19.2	34.9	6.8	44.2	43.3	3.4
11	TREM06	Tremedal 2nd Location			4440						
12	SARD02	Sardon Village			1440						
13	MU03	Muellesdes			2880						

Perm: Permeameter; DR: Double ring infiltration test; Beta: Soil drainage function coefficient

We can observe from the Table 5 that the first 10 records were derived from the samples of soil textural analysis, the remaining three points are locations where only double ring infiltration test were conducted. In addition values of saturated conductivity determined using SPAW are in the order from 724 to 1406 mm/d, however values estimated by double ring infiltration test were calculated over 3000 mm/d. This difference may be attributable to local fractures or a human error during the experiment. These results was combined with samples analyzed by Berhe (2010) in order to define Soil Map Class properties, The values are show in Appendix B-3.

### 5.1.5. Soil Class Map

The soil class map was derived from the geomorphologic map combined with information from the samples processed in the lab. Every map unit was characterized by the average of the soil properties established inside of them. The map units with their respective properties are shown in the Table 6, the class Id=40 was assigned to those grid cell corresponding to inselbergs and outcrops, so the properties were set equal to 0.

Table 6. Soil Classes with hydraulic properties

Id	Name	COD	POR	FC	WP	B	ksat01
10	Regolith	RE001	0.4185	0.1477	0.0610	3.719	1266.3
20	Regolith/Rock	RR002	0.4090	0.1290	0.0523	3.500	1400.7
30	Alluvium	AL003	0.4193	0.1020	0.0303	2.667	2067.9
40	Inselberg/Outcrops	NSOIL	0.0000	0.0000	0.0000	0.0000	0.0000

POR: Porosity; FC: Field Capacity; WP: Wilting point; B: soil drainage function coefficient (dimensionless); ksat01: Saturated hydraulic conductivity mm/d

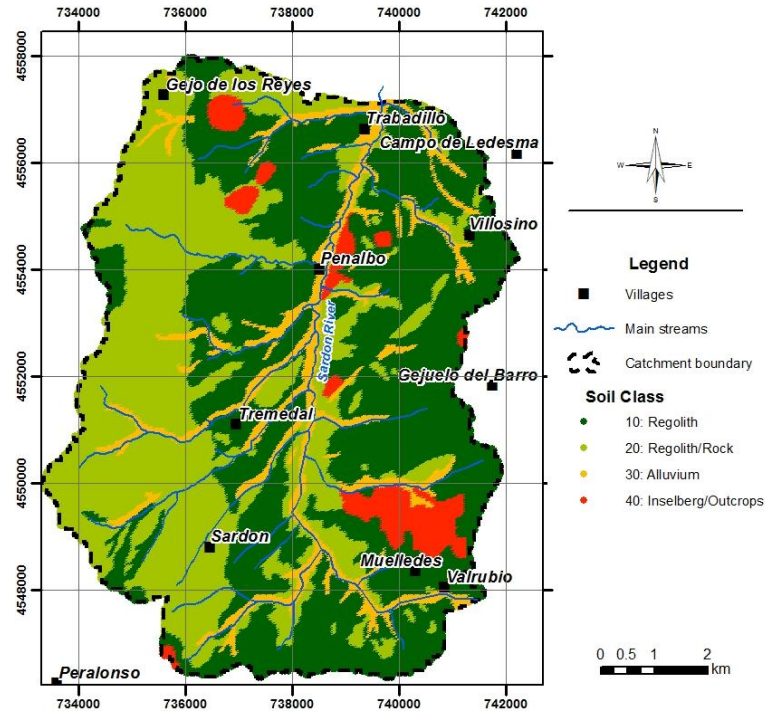


Figure 21. Soil depth map

### 5.1.6. Soil Depth Map

The soil depth map was developing after an interpolation of field observations combined with geomorphometry, then was evaluated with support of orthophotography. The interpolation was done using ordinary kriging method according to the procedure explain in the methodology, the semivariogram circular used had a partial sill =0.52 ; nugget= 0; and a range = 157. It is important to notice that this depth is relative to the values measured in field and to the methodology. Indeed more research about this topic is necessary in order to validate this procedure.

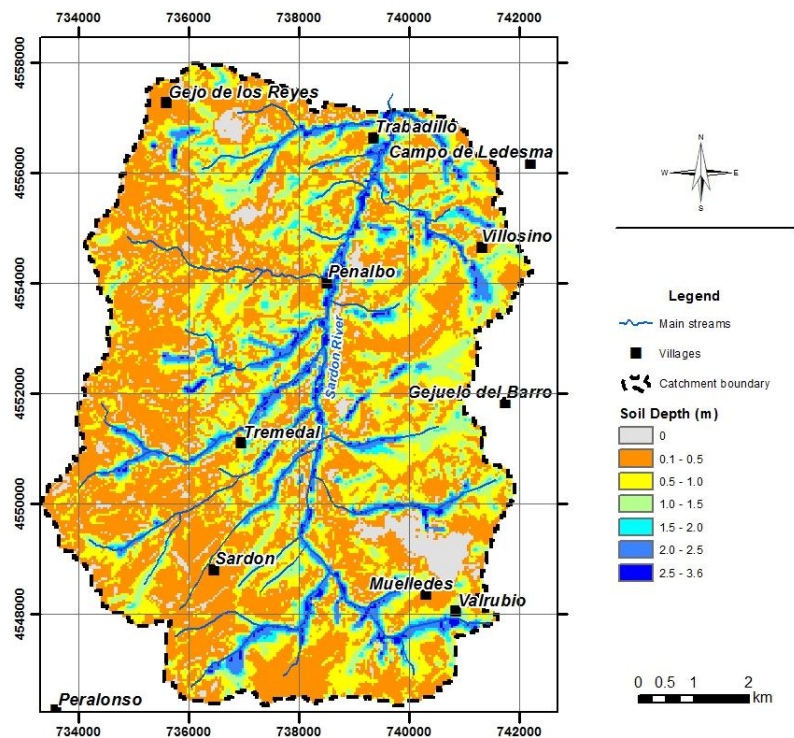
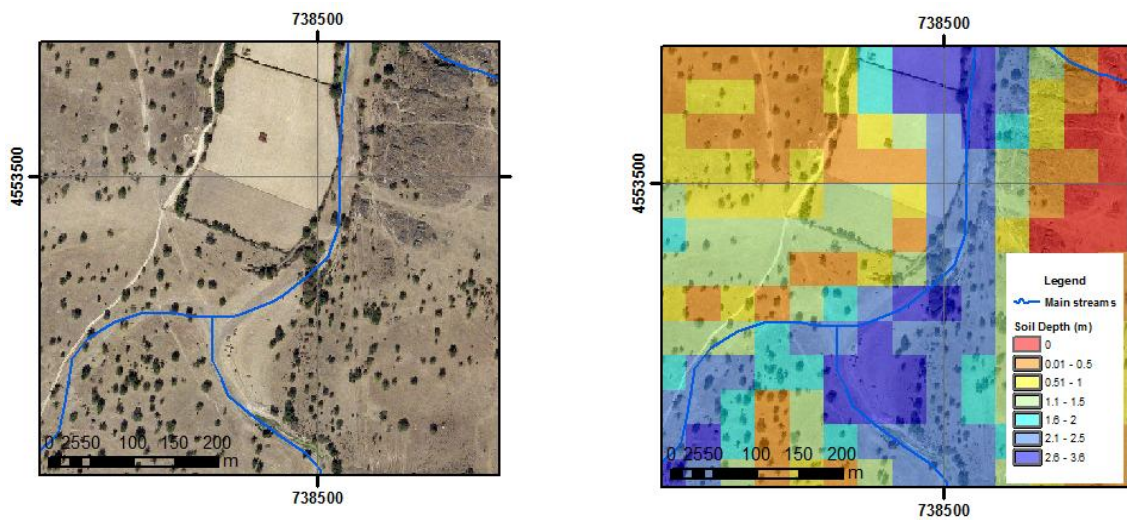
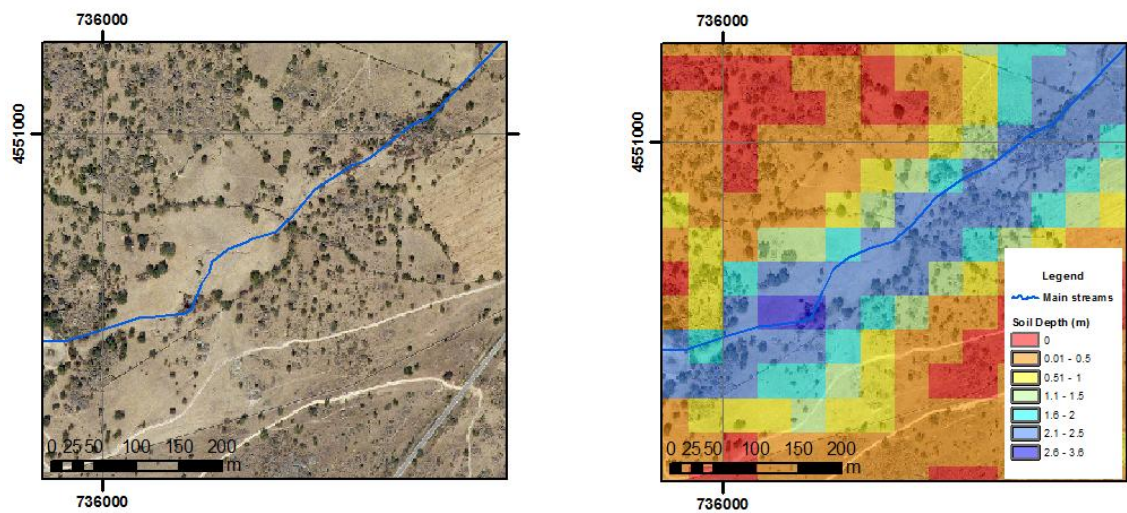


Figure 22. Soil depth map

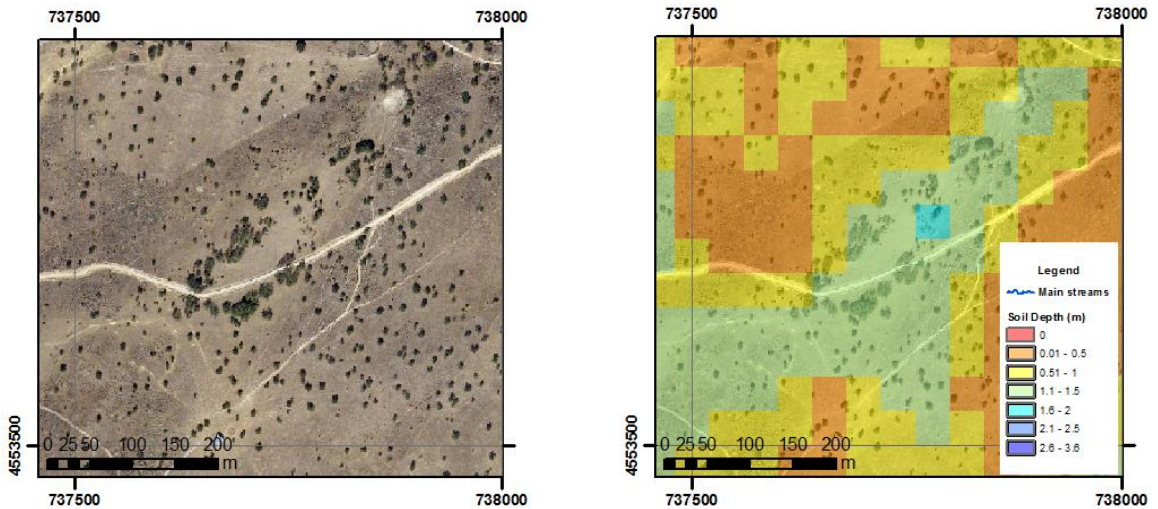
This method was used to represent the gradient of the soil depth, and it is based on relative representation of soil depth, in function of generic landforms, in order to evaluate the obtained values, a visual comparison was done. Three locations are illustrated in the Figure 23.



- a) The drainage channel in the left shows a mayor accumulation of alluvium material which correspond to a higher value of soil depth in the map at right side.



- b) The rocky area showed in the orthophoto at the upper left corner has a correspondent values equal or close zero in the representation in the at the map at right side



c) Even at places where drainage is not well defined the gradient seems to be adapted to the reality.

Figure 23. Visual evaluation of soil depth map using Orthophotography.

### 5.1.7. Bedrock Map

Bedrock map compiled from the study done by Tesfai (2000), it is shown in the Figure 24. For the present study values of saturated conductivity and porosity were assigned according to the Table 7:

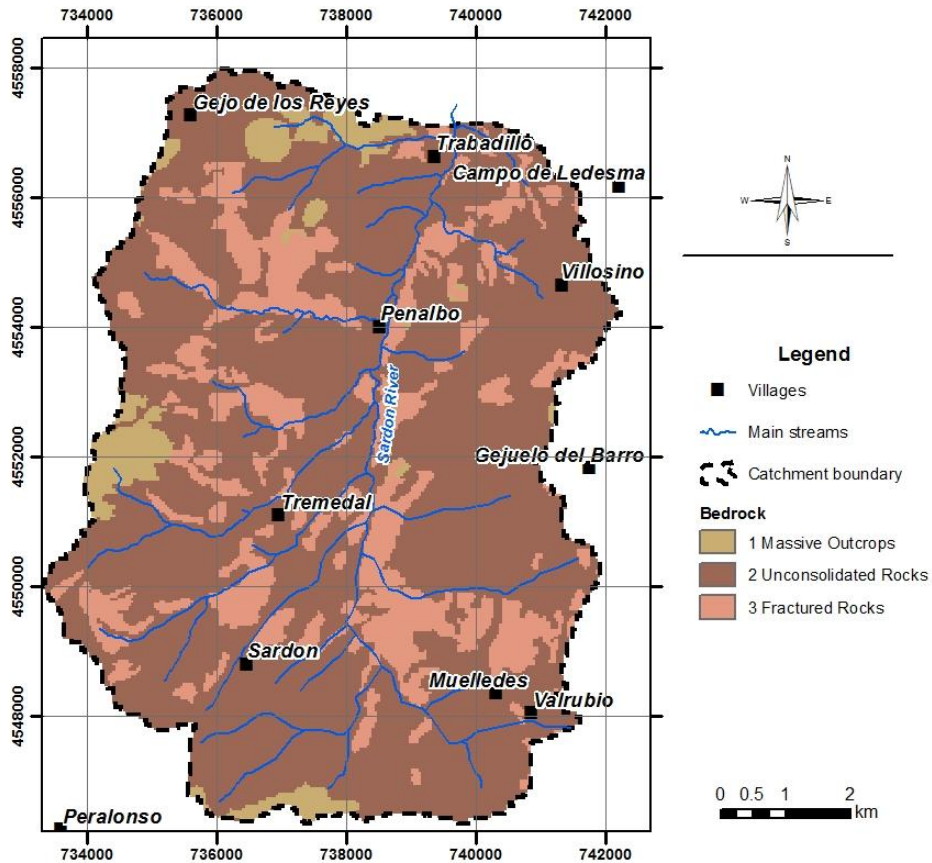


Figure 24. Bedrock map after (Tesfai, 2000)

Table 7. Hydraulic properties for the bedrock

Id	Name	POR	ksat(mm/d)
1	Massive outcrops	0.01	0.001
2	Unconsolidated Rocks	0.30	1.0
3	Fractured granite	0.1	0.1

POR: Porosity; Ksat: saturated vertical

These values have been adopted from the literature (see also, section 4.6), and even when they present a high level of uncertainty, they were for the simulation. Improving these parameters would be essential to improve the spatial distribution of recharge over the catchment.

### 5.1.8. Vegetation Map

INFIL3.0 requires a percentage of vegetation cover for each grid cell to be modelled, so this parameter was derived from the image classification done by Reyes (2011). The percentages of *Q. Ilex* and *Q. Pyrenaica* present in each grid cell are shown in colour scale in the Figure 25.

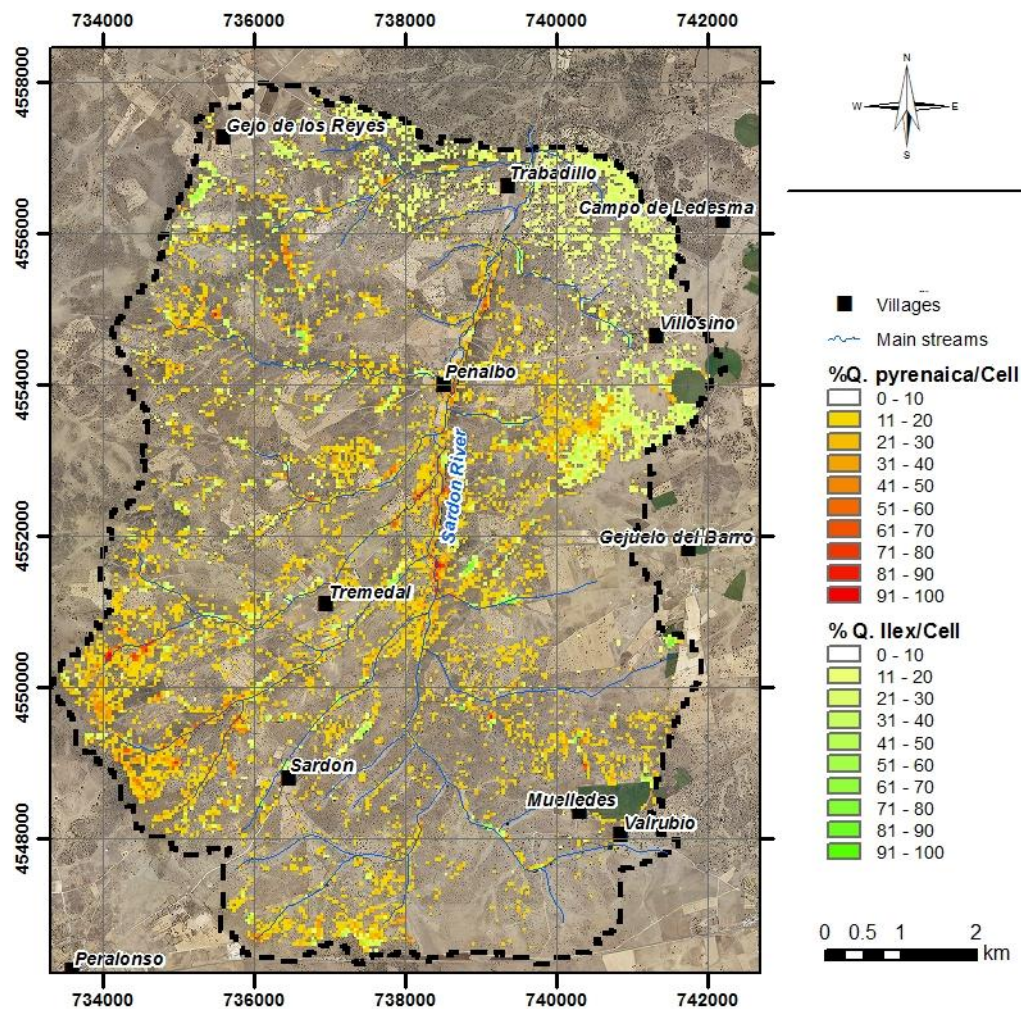


Figure 25. Vegetation Map in percentage of tree coverage per grid cell.

We can observe a high density of oak trees, following the drainage patterns with greater presence of *Q. Ilex* at the north-east part of the catchment and *Q. Pyrenaica*, at the south west part of the catchment.

## 5.2. Model simulations

Modelling has run considering for the period from Sep 2003 to Dec 2008, the period from Sep 2003 to Dec 2006 is used for warming up. The time step is equal to one day and most of the terms in the water balance of the model are given an initial condition of 0, and then continuously updated. However, initial conditions for water content of the five soil layers must be specified. In this study since the starting date of the simulation is a dry season, it was decided to select the option that set the water content of each layer as the product of wilting point and the thickness of each layer.

“Standard” conditions for some variables are established in the simulation follow:

Variable **sumbeg** and **sumend**, that defines the Julian day when summer starts and end, were set to 172 (21<sup>st</sup> June) to 266 (23 Sept) respectively. Also the duration of summer and winter storms were adopted with default values as 2h and 12h respectively.

Other initial value used by INFIL3.0 is the adjustment factor for potential evapotranspiration, the documentation of the model suggest to use equal to 0.15748 in arid to semi arid catchments. The multiplying factors used for calibration of INFIL3.0 (sdfact, pptfact, etfact,imbfact,sksfact) were set to 1 in order to not affect this standard results. Parameters that control surface water routing were configured as is shown in Table 8.

Table 8. Parameters that control surface water routine

ICHANMOD	CHAN1	CHAN2	CHAN3	CHAN4
1	0.20	500	0.8	1.0
IKSCHNMOD	KSCHN1	KSCHN2	KSCHN3	
0	500.0	2000.0	1.0	

## 5.3. Evaluation of the model

After the standard simulation with the conditions explained in the previous section two evaluations were done in order to analyze the behaviour of the model. Since data of streamflow suggested to calibrate the model were not available, first a comparison of actual and potential evapotranspiration (calculated with Priestley-Taylor equation) from eddy tower, and second, a evaluation of soil water content with the values obtained from water mark sensors installed near to Trabadillo station.

### 5.3.1. Comparison of the model with the footprint of Eddy Tower

To evaluate potential and actual evapotranspiration calculated by the model, data from the eddy tower installed near to Trabadillo ADAS station were used. Due to the fact that data from the tower were only available for 2010, and simulation was done for the period 2007-2008, comparison between 2010 and 2008 is not entirely correct, but it was the only option to evaluate this simulation.

Comparing evapotranspiration values require select the area equivalent to the footprint of the eddy tower (~500m). So grid cell pixel from the model founded in a radius of 500 m from the location of the tower was selected as adequate for this analysis. This radius corresponds to the average of the footprint area that contributes 80% of the measured flux (unpublished results, Van der Tol). The period selected is from February 2 to October 3 (according to data availability).

Figure 26, shown fluxes measured at the eddy tower; the precipitation for the year 2010 in the top graph and potential evapotranspiration calculated from Priestley Taylor equation (in red), and actual evapotranspiration (green) with some gaps interpolated (blue) in the bottom graph.

Evapotranspiration calculated with Priestley Taylor, varied between 0.16 mm/d to 6.14 mm/d. whilst actual evapotranspiration vary from 0.09 to 4.1 mm/d.

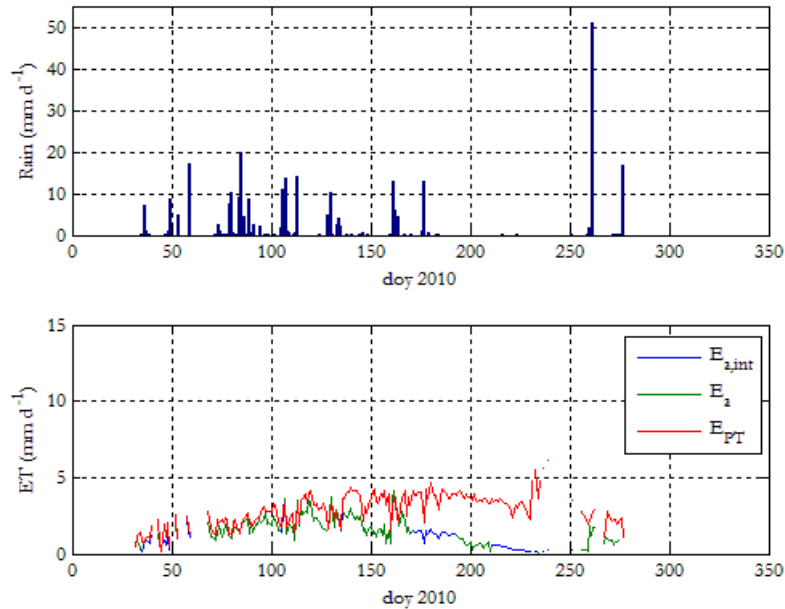


Figure 26. Fluxes precipitation and evapotranspiration, 2010 determined in the tower

Figure 27 shows the average of modelled daily data for the pixels around the tower, The figure shown values for Potential evapotranspiration calculated with Priestley Taylor equation (green) between 0.47 and 5.99mm/d. Values for actual evapotranspiration (blue) are between 0.038 and 5.6.

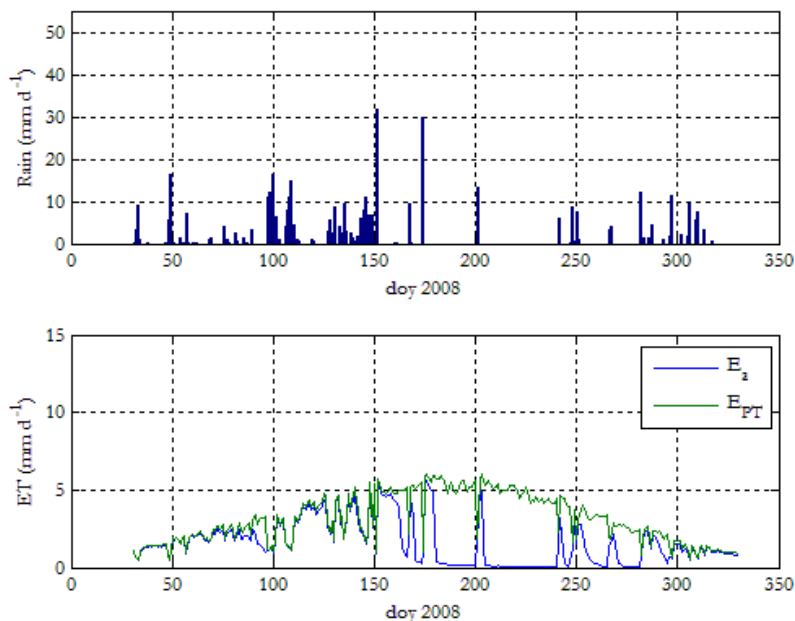


Figure 27. Fluxes precipitation and evapotranspiration, 2008 calculated by INIFIL3.0

Comparing Figure 26 and Figure 27 even when are from different years we can observe the same tendency. During the first days of the year in the rainy season values of Potential and actual evapotranspiration are quite similar, while in the dry period from day 175 to 250, actual evapotranspiration calculated by INFIL3.0 decrease drastically to values close to 0. Comparing with values estimated in the tower for a similar dry period, actual evapotranspiration do no present same decrease. We could say that INFIL3.0 for dry seasons is not simulating adequately actual evapotranspiration for dry seasons. If we had the same period of data availability, then this procedure would have been a quite good tool to fit model simulations. A possible reason why INFIL3.0 gives too little actual evapotranspiration values could be the transpiration of groundwater by oak tree species is not being considered.

With this analysis at least we can see that potential evapotranspiration simulated was acceptable, and response of actual evapotranspiration after rainfall and during the dry season was realistic.

Also cumulative fluxes for precipitation and actual evapotranspiration for 2008 and 2010 were checked and shown in the Figure 28. We can observe the period from the day of year (DOY) 33 to 150, in the graph of modelled data (2008), precipitation and actual evapotranspiration are quite similar, with few periods where precipitation is bigger. The cumulative measured precipitation (2010) is initially higher than actual evapotranspiration, but after DOY 150 evapotranspiration overtakes precipitation and actual evapotranspiration curves.

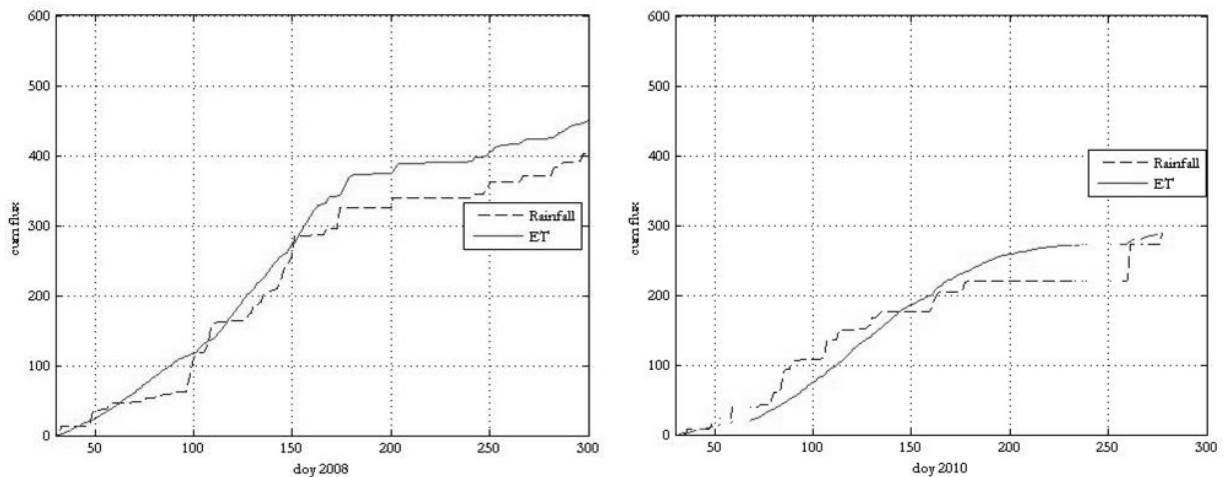


Figure 28. Comparing cumulative fluxes for precipitation and actual evapotranspiration for the years 2008 (left) and 2010 (right)

Cummulative precipitation and evapotranspiration is an important quantity, because it is the replenishment of the soil and it should affect recharge. In both cases (modelling and measured) it is rather small, and thus the recharge could also be going to be small.

### 5.3.2. Comparison with soil moisture profiles

The second way to evaluate results of modelling was to compare soil water content derived from matric potential sensors installed close to Trabadillo ADAS station with simulated time series of water content in through different soil layers discretized for the correspondent position. For the sensor located under the *Q.Pyrenaica* tree and for the close pixel.

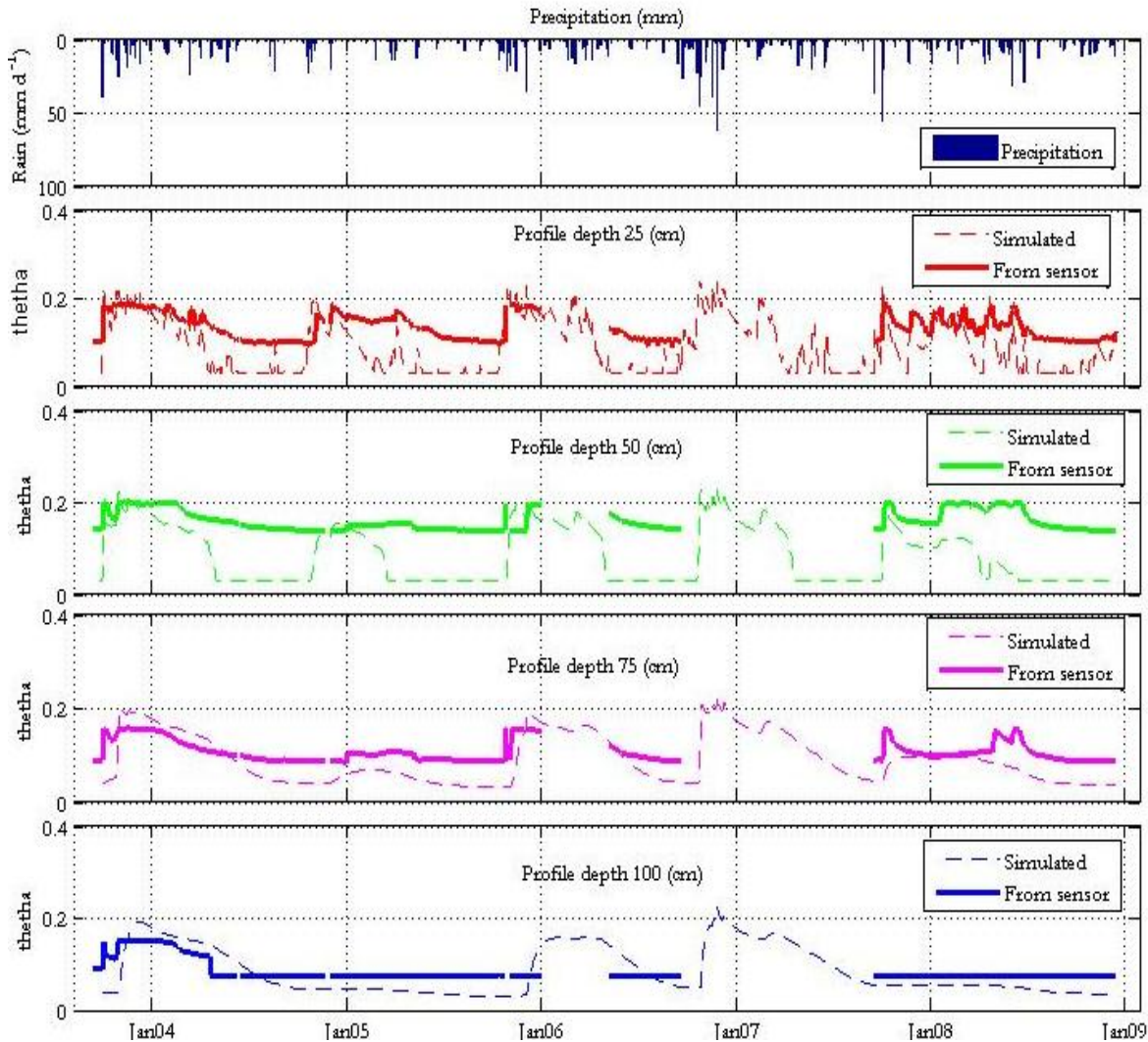


Figure 29. Soil moisture profiles. Thick lines represent values of soil moisture converted from matric potential sensor installed under *Q. Pyrenaica* tree, and segmented line represent values simulated from the model for corresponding pixel location.

Although exist uncertainties in the determination of moisture in the profile and the scale of comparing one grid cell with the soil profile measured at a point could not be adequate, we can observe the similar trend in the profiles.

Taking a closer look at the case of the shallowest profile (at a depth 25 cm) in Figure 30, shows that the that the response of modelled and measured soil moisture to precipitation is quite similar.. Because INFIL model is the bucket type each layer works as a reservoir which is filled and emptying according to the time step and following the equations that control the drainage between layers. The similar response shows that this bucket model was sufficiently well parameterized.

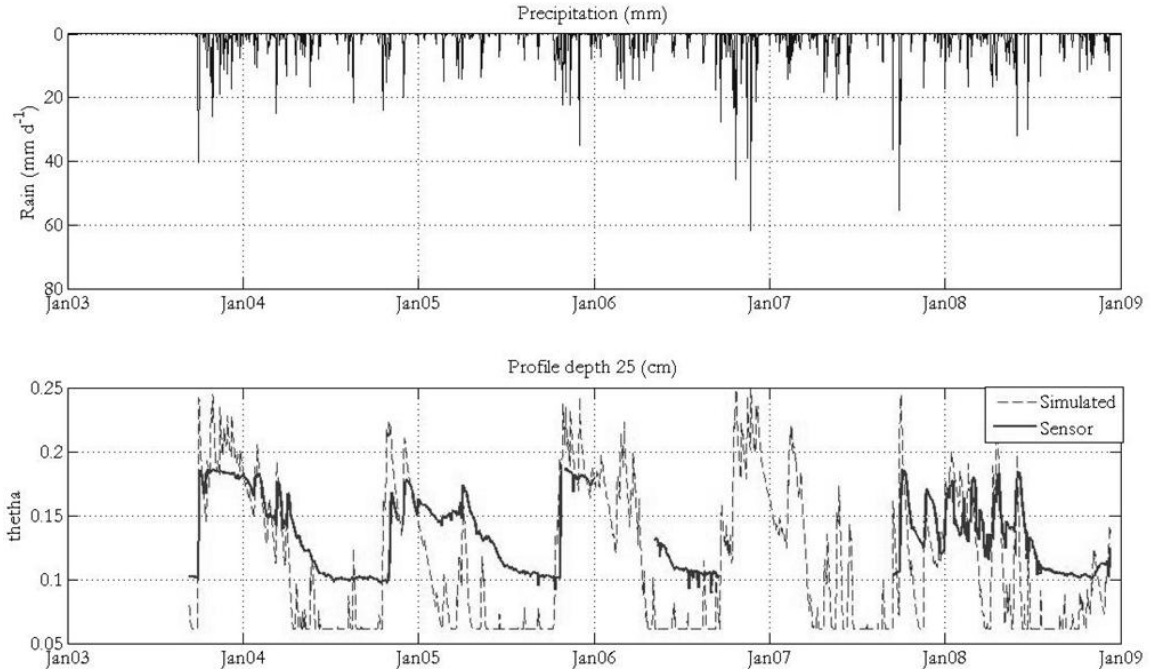


Figure 30. Soil water content simulated and calculated from matric potential sensor at 25 (cm)

#### 5.4. Results of model simulation

For the averaging period from January, 2007 through December, 2008 discarding the years of warming up, results shown in the summary output file indicate that the precipitation was 515.7 mm/year, also the average annual actual evapotranspiration within the soil zone, 430.8 mm/year it is about 41.8 % of the potential evapotranspiration within the watershed (1031.28mm/year). The results of the root zone mass balance are graphically represented in the following figure:

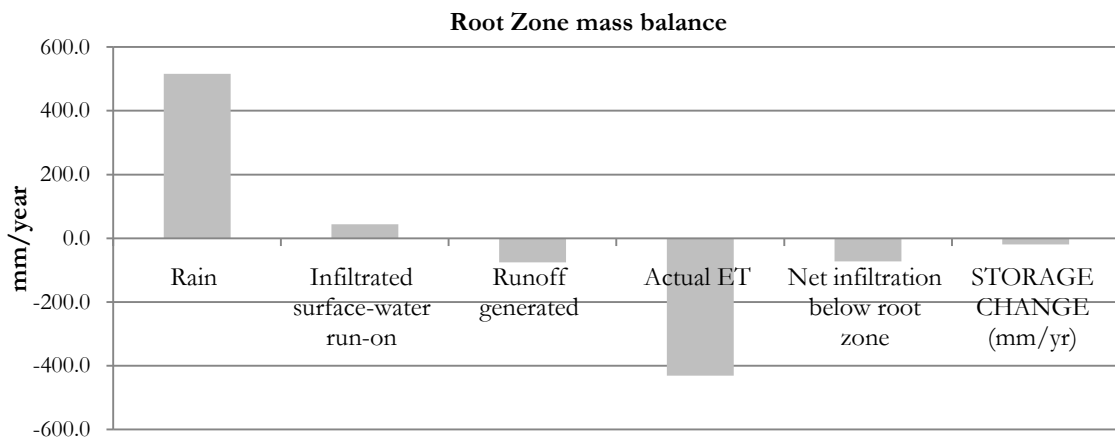


Figure 31. Root zone mass balance

We can observe that average annual Net infiltration below root zone or potential recharge is 72.3 mm/year, expressed as a percentage of rain is equal to 14%.

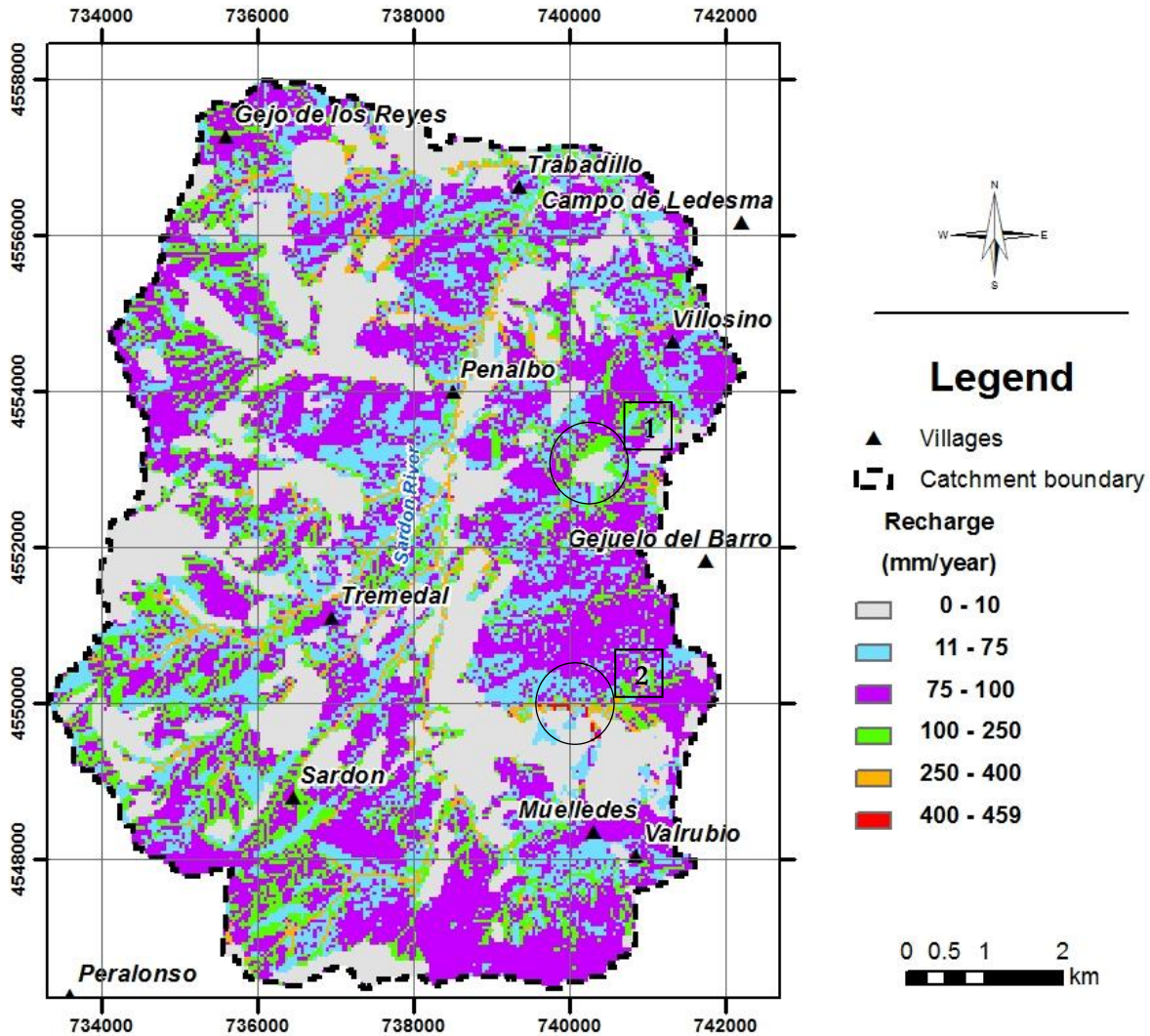


Figure 32. Recharge Map (mm/year)

The map with the average annual recharge calculated is in the Figure 32. Results obtained indicate pixels with higher values of infiltrations are located over the drainage network with values between 250 and 400 mm/year (probably model outliers in geo-contacts), while the lower values of recharge in gray are related with areas of massive and fractured granite outcrops.

Pixels in green with a relatively high recharge are related to neighbouring areas of outcrops, this is because run off coming from outcrops readily infiltrates into the higher permeability cells downstream this can be observed in the place marked with the number 1 at the Figure 32.

The highest values of infiltration are for those pixels indicated with the number 2 at the Figure 32, they seem to have the combined effect of being part of the drainage area, to be close a rocky area, and also classified within a soil class with high vertical hydraulic conductivity.

Cell grids in cyan and magenta, occupying a big percentage of the catchment area, are quite similar to the average value (72.3 mm/year) calculated for the simulation period.

Furthermore we have to said that the high values of recharge located over the stream area could be explained since INFIL3.0 uses a routine that enhance infiltration over channels by controlling vertical

hydraulic conductivity of a grid cell as a function of number of pixels flowing into them from the upstream area. In the present study this parameters were configured according the documentation of the model and values were assigned according to the Table 8. However it is necessary more research about their influence on the spatial distribution of the recharge.

#### 5.4.1. Comparison with previous studies

A recompilation of groundwater recharge estimations obtained from previous studies is shown in Table 9. With the objective of compare estimated values from INFIL3.0 with information of previous studies, a map of groundwater recharge in percent of rainfall was created and is shown in the Figure 33.

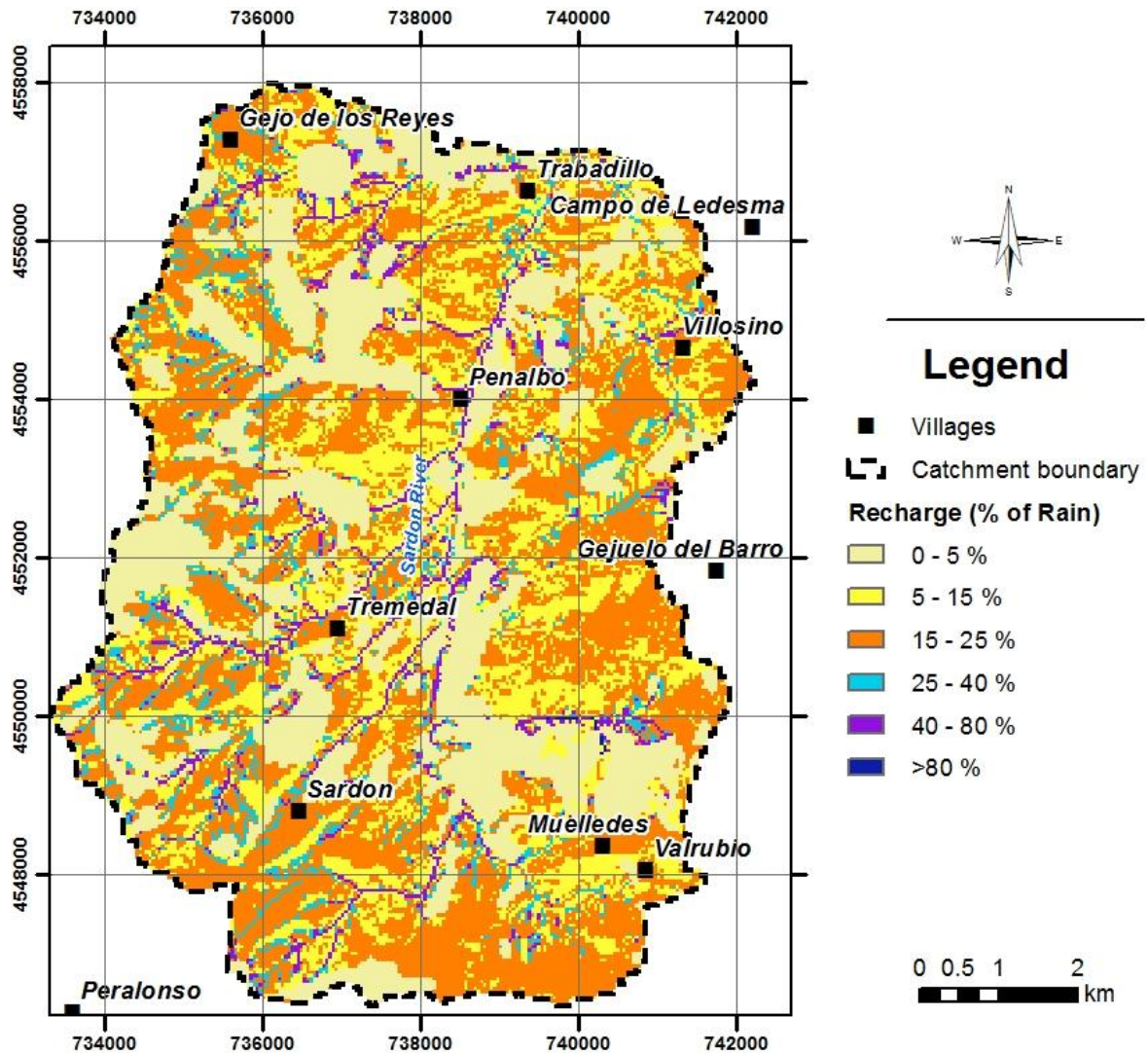


Figure 33. Recharge in percentage of rainfall for the period 2007 to 2008

Table 9. Values of recharge calculated in previous studies

MODFLOW - Steady State				MODFLOW - Transient				
Previous Studies	Period	Recharge mm/year	RF%	Recharge RF%				
Ruwan (2009)	2003-2008	70,7	12.3%	24.1				
Lubczynski and Gurwin (2005)	1996-2000	56	11%	24.5				

pyEarth-1D				Chloride mass balance (CMB)					
Previous Studies	Period	Recharge RF%				Recharge RF%			
		Pt.	min	max	average	Pt.	min	max	average
Ruwan (2009)	2003-2008	6	10.4	29.3	20.5	6	4.2	19.3	10.5
<b>Earth-1D</b>									
Uria (2000)	1998 -1999	6	8.6	36.4	18.4	5	17.8	75	48.2

Pt: Number of points evaluated

Reviewing Table 9, results of simulated recharge for the period 2007-2008 with INFIL3.0 are more similar to the values calculated by Ruwan (2009) (12.3%RF) for simulations in MODFLOW in the steady state, a possible reason is that the period of study and meteorological data used were the same. However in MODFLOW transient mode these values are different, 24.1%RF compared with the average value of 14%RF obtained with INFIL3.0. A similar situation is observed comparing with results from Lubczynski and Gurwin (2005), the 11%RF in Steady state is closer than the estimated in transient mode.

Comparing with values of pyEarth simulations from Ruwan, an average of 20.5%RF is estimated, but this value is influenced for the positions where simulations were done, to improve this comparison should be better to evaluate the geographical positions, but meanwhile we could said that average annual value estimated by INFIL3.0 is within the minimum and maximum estimated by pyEarth1D, 10.4% and 29.3%RF respectively.

Following with chloride mass balance method, values estimated by Uria(2000) are the biggest, 75%RF, but it was explained on that study that the reason for this overestimation was a high chloride content in the rain water. In the case of Ruwan, results of chloride mass balance method (CMB) shows values between 4.2%RF and 19.3%RF, and are relatively comparables with the areas in yellow colour in the recharge map

## 6. CONCLUSIONS AND RECOMENDATIONS

There are many techniques to quantify ground water recharge in semiarid catchments. This research attempted to use the distributed-parameter water-balance model INFIL3.0 in the Sardon catchment as a complementary method to the former studies.

A procedure based on the geomorphologic map combined with generic landforms is used to estimate a distributed map of soil depth. This procedure based on GIS techniques demonstrates to be an alternative to estimate soil depth.

Soil hydraulic properties were spatially distributed over geomorphologic units with data obtained from fieldwork and laboratory methods.

Percentage of vegetation cover of each grid cell of the model is very well characterized by using a GIS methodology and a high resolution classified image as input.

The proposed procedure to evaluate the simulation supported by data of evapotranspiration from eddy tower was adequate for the conditions of this study, and could be improved if time series would be available for the same simulation period.

The simulation of groundwater recharge with INFIL 3.0 presents a yearly average value of 72 mm/year equivalent to 14% of the rainfall, for the period from January 2007 till December 2008. Spatial distribution varies from higher values located over stream channels (>80%RF) and close to outcrops (15-40%), and very low values of recharge for areas of surface presence of massive and fractured granite (0-5%). These values are indicative in the absence of calibration records.

Taking in account that former studies have determined ground water recharge at different temporal and spatial scales, the estimated value of 14% of rainfall as groundwater recharge compared well to those values calculated in simulation in MODFLOW steady state simulation 12.3%RF Ruwan (2009).

Estimations of recharge calculated by Earth1D model resulted in higher values than the average yearly determined by INFIL3.0, while average recharge calculated by CMB method from Ruwan (2009) is lower.

Although similar estimations of ground water recharge were found comparing with other methods of estimation, is difficult to assess if INFIL3.0 is a reliable method to estimate ground water recharge without model calibration..

### **Recomendations:**

The software documentation indicates the need of at least: maximum daily discharge, annual discharge, monthly discharge, streamflow discharge, and daily discharge in order to perform model calibration. This data was not available for Sardon.

An alternative calibration could be if the recharge estimates are used in a ground-water-flow model calibrated to water-level data and known discharges for the area of interest.

During the simulation it was detected a strong influence of soil depth, bedrock hydraulic conductivity, winter and summer storm durations. A sensitivity analysis could not be performed due to time constrictions but this procedure is highly recommended.

Spatial variability of soil properties can be improved by means of techniques that are based on regression-kriging where the principle is to employ most of the available regression and kriging benefits.

## LIST OF REFERENCES

---

- Allen, R. G., and FAO. (1998). *Crop evapotranspiration : guidelines for computing crop water requirements*. Rome: FAO.
- Berhe, E. T. (2010). *Improving groundwater model reliability by coupling unsaturated and saturated models : a case study of Sardon catchment, Spain*. Unpublished MSc Thesis, ITC, Enschede.
- Campbell, G. S. (1985). *Soil physics with BASIC : transport models for soil - plant systems*. Amsterdam etc.: Elsevier.
- Canadell, J., Jackson, R. B., et al. (1996). Maximum rooting depth of vegetation types at the global scale. *Oecologia*, 108(4), 583-595.
- de Bruin, H. A. R. (1988). Evaporation in arid and semi-arid regions. In I. Simmers (Ed.), *Estimation of natural groundwater recharge* (pp. 73–88). Boston: Reidel Publishing Company.
- Dobos, E., and Hengl, T. (2009). Chapter 20 Soil Mapping Applications. In H. Tomislav & I. R. Hannes (Eds.), *Developments in Soil Science* (Vol. Volume 33, pp. 461-479): Elsevier.
- Eijkelkamp.com. (2010). Laboratory Permeameter Operating Instructions. from <http://www.eijkelkamp.com/Portals/2/Eijkelkamp/Files/Manuals/M1-0902e%20Lab-permeameters.pdf>
- FAO. (1974). *Soil survey in irrigation investigations*. Rome: FAO.
- Flint, A. L., and Childs, S. W. (1987). Calculation of solar radiation in mountainous terrain. [doi: DOI: 10.1016/0168-1923(87)90061-X]. *Agricultural and Forest Meteorology*, 40(3), 233-249.
- Gobin, A., Campling, P., et al. (2001). Soil-landscape modelling to quantify spatial variability of soil texture. [doi: DOI: 10.1016/S1464-1909(01)85012-7]. *Physics and Chemistry of the Earth, Part B: Hydrology, Oceans and Atmosphere*, 26(1), 41-45.
- Grunwald, S. (2006). *Environmental soil-landscape modeling: geographic information technologies and pedometrics*: CRC/Taylor & Francis.
- Hengl, T. (2006). Finding the right pixel size. [doi: DOI: 10.1016/j.cageo.2005.11.008]. *Computers & Geosciences*, 32(9), 1283-1298.
- Hengl, T., and Reuter, H. I. (Eds.). (2009). *Geomorphometry : concept, software, applications*. Amsterdam: Elsevier Science.
- Hernández, V., Martínez, J., et al. (2008). Response of *Quercus pyrenaica* (melojo oak) to soil water deficit: a case study in Spain *European Journal of Forest Research*, 127(5), 369-378.
- Hevesi, J. A., Flint, A. L., et al. (2003). Simulation of net infiltration and potential recharge using a distributed-parameter watershed model of the Death Valley region, Nevada and California.U.S. Geological Survey Water-Resources Investigations Report 03–4090.171 p
- IGME (1991a). *Mapa Geomorfológico de España, Hoja 451 (Ledesma)*. Instituto Tecnológico Geominero España
- IGME (1991b). *Mapa Geomorfológico de España. Hoja 450 (Vitigudino)*.
- Iqbal, M. (1983). *An introduction to solar radiation*: Academic Press.
- Jury, W. A., Gardner, W. R., et al. (1991). *Soil physics* (Fifth edition ed.). New York etc.: Wiley & Sons.
- López, B., Sabaté, S., et al. (2001). Vertical distribution of fine root density, length density, area index and mean diameter in a *Quercus ilex* forest. *Tree Physiology*, 21(8), 555-560.
- Lubczynski, M. W., and Gurwin, J. (2005). Integration of various data sources for transient groundwater modeling with spatio-temporally variable fluxes--Sardon study case, Spain. [doi: DOI: 10.1016/j.jhydrol.2004.08.038]. *Journal of Hydrology*, 306(1-4), 71-96.
- Maidment, D. R. e. (2002). *Arc hydro : GIS for water resources*. Redlands: ESRI.
- McBratney, A. B., Odeh, I. O. A., et al. (2000). An overview of pedometric techniques for use in soil survey. [doi: DOI: 10.1016/S0016-7061(00)00043-4]. *Geoderma*, 97(3-4), 293-327.
- NASA. (2011a). Aerosol Robotic Network AERONET. from <http://aeronet.gsfc.nasa.gov/>
- NASA. (2011b). Total Ozone Mapping Spectrometer. from [http://toms.gsfc.nasa.gov/ozone/ozone\\_v8.html](http://toms.gsfc.nasa.gov/ozone/ozone_v8.html)
- Nishikawa, T., Izbicki, J. A., et al. (2004). Evaluation of geohydrologic framework, recharge estimates, and ground-water flow of the Joshua Tree area, San Bernardino County, California: U.S. Geological Survey Scientific Investigations Report 2004–5267115 p
- Rewis, D. L., Christensen, A. H., et al. (2006). Geology, ground-water hydrology, geochemistry, and groundwater simulation of the Beaumont and Banning storage units, San Geronio Pass area,

Riverside County. California: U.S. Geological Survey Scientific Investigations Report 2006–5026173 p

- Reyes, L. J., and Lubczynski, M. W. (2011). Spatial assessment of transpiration, groundwater and soil-water uptake by Oak trees in dry-season at a semi-arid open-forest in Salamanca, Spain. *in press*.
- Ruwan Rajapakse, G. (2009). *Numerical groundwater flow and solute transport modelling : a case study of Sardon catchment in Spain*. ITC, Enschede.
- Sanford, W. (2002). Recharge and groundwater models: an overview. *Hydrogeology Journal*, 10(1), 110-120.
- Scanlon, B. R., Healy, R., et al. (2002). Choosing appropriate techniques for quantifying groundwater recharge. *Hydrogeology Journal*, 10(1), 18-39.
- Scanlon, B. R., Keese, K. E., et al. (2006). Global synthesis of groundwater recharge in semiarid and arid regions. [Review]. *Hydrological Processes*, 20(15), 3335-3370.
- Shakya, D. R. (2001). *Spatial and temporal groundwater modeling integrated with remote sensing and GIS : hard rock experimental catchment, Sardon, Spain*. Unpublished MSC Thesis, ITC, Enschede.
- Shuttleworth, J. M. (1993). Evaporation. In D. R. Maidment (Ed.), *Handbook of hydrology* (pp. 650). New York etc.: McGraw-Hill.
- Silva, J. S., Rego, F. C., et al. (2003). Root distribution of Mediterranean woody plants. Introducing a new empirical model. *Plant Biosystems - An International Journal Dealing with all Aspects of Plant Biology: Official Journal of the Societa Botanica Italiana*, 137(1), 63 - 72.
- Stannard, D. I. (1993). Comparison of Penman-Monteith, Shuttleworth-Wallace, and modified Priestley-Taylor evapotranspiration models for wildland vegetation in semiarid rangeland. *Water Resources Research*, 29(5), 1379-1392.
- Stasko, S., Tarka, R., et al. (2008). Groundwater recharge in mountainous terrains : case study from Sudeten mountains in SW Poland. In: *Global groundwater resources and management : selected papers from the 33rd International Geological Congress (IGR), Oslo, Norway, 6-14 August 2008 / ed. by B.S. Palival. Jodhpur : Scientific Publishers, 2008. pp. 451-474*.
- Tesfai, B. H. (2000). *Subsurface characterization of granitic basement from structural and resistivity data : a case study from Sardon catchment area, Salamanca, Spain*. ITC, Enschede.
- U.S.G.S. (2008). Documentation of computer program INFIL3.0—A distributed-parameter watershed model to estimate net infiltration below the root zone: U.S. Geological Survey Scientific Investigations Report 2008–5006: U.S. Geological Survey. U. S. G. Survey.98 p
- Uria Cornejo, S. P. (2000). *Groundwater recharge modelling in hard rocks area : Sardon case study, Spain*. Unpublished MSc Thesis, ITC, Enschede.
- van Reeuwijk, L. P. (2002). Procedures for Soil Analysis (Sixth edition ed.): ISRIC & FAO Technical Paper 9.
- Vrba, J., and Lipponen, A. (2007). Groundwater resources sustainability indicators: UNESCO/IAEA/IAH Groundwater Indicators Working Group.I.-V. s. o. groundwater.
- W. Lubczynski, M., and Gurwin, J. (2005). Integration of various data sources for transient groundwater modeling with spatio-temporally variable fluxes--Sardon study case, Spain. [doi: DOI: 10.1016/j.jhydrol.2004.08.038]. *Journal of Hydrology*, 306(1-4), 71-96.

## APPENDIX A

---

### APPENDIX A- 1.Daily precipitation file format Sample:

daynumb	year	mon	day	ydy	1
1	2000	1	1	1	-999.99
2	2000	1	2	2	-999.99
3	2000	1	3	3	-999.99
4	2000	1	4	4	-999.99
5	2000	1	5	5	-999.99
6	2000	1	6	6	-999.99
7	2000	1	7	7	-999.99
8	2000	1	8	8	-999.99

.....  
Several lines of input deleted  
.....

1586	2004	5	4	125	0.44
1587	2004	5	5	126	6.69
1588	2004	5	6	127	0.21
1589	2004	5	7	128	0
1590	2004	5	8	129	0.14
1591	2004	5	9	130	7.11
1592	2004	5	10	131	0.5
1593	2004	5	11	132	0.55

### APPENDIX A-2. Monthly Atmospheric Parameters File:

ATMOS routine parameters  
file atmos.inp  
.....

month	ozone	wp	beta	csr	pg
1	0.29	0.870	0.061	0.50	0.22
2	0.29	1.010	0.044	0.50	0.20
3	0.33	0.840	0.042	0.50	0.21
4	0.41	1.400	0.078	0.50	0.22
5	0.36	1.400	0.048	0.50	0.22
6	0.33	1.500	0.050	0.50	0.22
7	0.29	1.600	0.040	0.50	0.23
8	0.33	1.720	0.040	0.50	0.24
9	0.31	1.820	0.093	0.50	0.21
10	0.26	1.510	0.040	0.50	0.22
11	0.30	0.920	0.022	0.50	0.22
12	0.25	0.950	0.022	0.50	0.22

## APPENDIX B

### APPENDIX B- 1. List of coordinates of soil samples taken during fieldwork campaign

<b>COD</b>	<b>DESC</b>	<b>DATE</b>	<b>XUTMW</b>	<b>YUTMW</b>	<b>RINGS</b>	<b>BAGS</b>
<b>TB01</b>	Trabadillo La Mata	08.09.2010	739653	4555667	1	0
<b>TB02</b>	Trabadillo La Mata	08.09.2010	739679	4555746	1	0
<b>LMAL03</b>	Los Malones	08.09.2010	735460	4548868	2	1
<b>TB05B1</b>	Trabadillo La Mata	09.09.2010	739657	4555673	0	1
<b>TB06B1</b>	North boundary of La Mata	09.09.2010	739652	4555749	0	1
<b>TB08R</b>	Trabadillo	09.09.2010	739140	4555870	2	0
<b>SVillo01</b>	Villosino	10.09.2010	740452	4555232	1	0
<b>SVillo02</b>	Villosino	10.09.2010	740348	4555212	2	3
<b>SPEN01</b>	Penalbo	11.09.2010	737324	4553383	3	3
<b>TREM01</b>	Tremedal	14.09.2010	737291	4551392	0	4
<b>GEJOR01</b>	Gejo de los Reyes	15.09.2010	736383	4555557	0	4
<b>TRABSS</b>	Trabadillo / Albarranes	15.09.2010	738522	4556380	0	3
<b>TBSTA30</b>	Trabadillo near station	16.09.2010	739368	4555676	0	11
<b>GEJOB</b>	Gejuelo del Barro	22.09.2010	739479	4551461	0	2
<b>GD1.2</b>	Trabadillo - La Mata	09.09.2010	739381	4555666	1	0
<b>GD3.1</b>	Trabadillo - La Mata	11.09.2010	739386	4555380	1	0
<b>GD1.1</b>	Trabadillo - La Mata	09.09.2010	739381	4555666	1	0
<b>GD2.1</b>	Trabadillo - La Mata	09.09.2010	739353	4555611	1	0
				Total	16	33

### APPENDIX B- 2. List of site coordinates of double ring test

<b>COD</b>	<b>Reference Place</b>	<b>Outer ring</b>	<b>Inner Ring</b>	<b>DATE</b>	<b>XUTMW</b>	<b>YUTMW</b>	<b>ELEV/GPS</b>
<b>LMAL03</b>	Los Malones	55	30	08.09.2010	735460	4548868	802
<b>LMAL01</b>	Los Malones	53	28	08.09.2010	735445	4548868	809
<b>TB06B1</b>	Trabadillo	57	28	09.09.2010	739652	4555749	743
<b>TB05B1</b>	Trabadillo	57	32	09.09.2010	739658	4555672	752
<b>TREM01</b>	Tremedal	53	28	14.09.2010	737291	4551392	763
<b>TREM02</b>	Tremedal	53	28	14.09.2010	737212	4551467	753
<b>TREM03</b>	Tremedal	53	28	14.09.2010	737235	4551459	766
<b>TREM04</b>	Tremedal	55	28	14.09.2010	737261	4551406	754
<b>TREM05</b>	Tremedal	53	28	14.09.2010	737303	4551390	732
<b>TREM06</b>	Tremedal	53	28	14.09.2010	737235	4551471	730
<b>SPEN1</b>	Penalbo	53	28	15.09.2010	737334	4553373	771
<b>SPEN2</b>	Penalbo	55	30	15.09.2010	737328	4553378	
<b>GEJOR01</b>	Gejo de los Reyes	53	28	15.09.2010	736383	4555557	764
<b>GEJOR02</b>	Gejo de los Reyes	55	30	15.09.2010	736384	4555504	
<b>TRABSS</b>	Trabadillo near Albarranes	55	30	15.09.2010	738522	4556380	755
<b>TRABSS02</b>	Trabadillo near Albarranes	57	32	15.09.2010	738529	4556395	746
<b>SARD01</b>	Sardon	55	30	17.09.2010	736108	4548304	827

COD	Reference Place	Outer ring	Inner Ring	DATE	XUTMW	YUTMW	ELEV/GPS
SARD02	Sardon	57	32	17.09.2010	736122	4548294	823
MU02	Near of Muelledes	55	30	17.09.2010	739697	4546864	820
MU03	Near of Muelledes	55	30	17.09.2010	739702	4546875	827
GEJOB	Gejuelo del Barro	57	32	16.09.2010	739420	4551491	667

### APPENDIX B- 3 Lab result for soil particle discrimination

ID	Depth (cm)	GRAVEL			SAND			SILT		CLAY
		>2mm	1.0-2.0 mm	0.5-1.0mm	250-500µm	100-250µm	50-100µm	20-50 µm	2-20 µm	< 2µm
LMAL03	(12)	9.3	19.7	13.6	10.8	14.6	8.5	5.6	11.4	6.5
TB05B1	(10)	16.6	20.8	16.6	13.9	13.1	4.6	3.3	5.9	5.2
TB06B1	(10)	3.0	10.1	25.2	16.5	10.0	2.4	4.1	14.1	14.5
TREMSS-01	(20)	8.2	19.4	18.1	12.4	10.1	4.3	6.0	13.0	8.4
TREMSS-02	(50)	8.3	14.5	17.5	16.1	15.1	5.9	6.8	11.3	4.6
TREMSS-03	(80)	12.0	25.4	22.5	17.5	11.3	3.0	1.9	3.2	3.2
TREMSS-04	(100)	17.7	27.5	21.4	15.0	9.6	2.7	1.2	3.0	2.0
GEJOR-01	(20)	11.2	19.0	13.5	11.2	11.4	5.7	4.6	13.3	10.2
GEJOR-02	(50)	6.3	14.4	15.4	13.4	14.3	6.3	6.1	13.3	10.5
GEJOR-03	(80)	16.1	20.8	15.2	12.5	12.8	4.6	2.6	6.2	9.2
GEJOR-04	(100)	8.5	18.8	16.9	15.8	16.5	6.1	5.4	6.8	5.2
TRSS1	(20)	6.5	14.9	15.3	9.8	7.9	3.6	7.5	21.6	12.8
TRSS2	(50)	7.9	16.4	18.1	11.3	9.4	4.0	6.3	14.9	11.6
TRSS3	(80)	16.4	18.3	14.7	11.2	9.9	3.7	6.3	10.3	9.1
TBSTA30-1	(20)	15.4	19.4	15.7	10.8	10.5	4.5	4.2	10.6	9.0
TBSTA30-2	(40)	21.2	21.7	15.0	9.4	10.0	4.2	3.7	7.9	6.8
TBSTA30-3	(60)	9.5	18.3	14.2	10.2	11.8	6.3	7.2	14.0	8.5
TBSTA30-4	(80)	20.2	12.5	9.9	8.2	15.3	7.9	5.6	12.1	8.3
TBSTA30-5	(100)	20.7	17.4	10.5	8.3	14.5	7.9	5.8	9.0	5.8
TBSTA30-6	(150)	32.6	19.5	11.3	7.0	8.8	3.9	11.6	3.2	2.0
TBSTA30-7	(170)	32.0	23.5	14.6	8.7	8.6	3.8	2.3	3.8	2.6
TBSTA30-8	(200)	22.2	14.0	16.1	14.5	16.4	5.7	2.9	5.0	3.4
TBSTA30-9	(220)	13.8	13.2	17.0	17.9	19.5	6.4	3.0	5.1	4.2
TBSTA30-10	(250)	19.9	17.5	12.6	14.9	17.7	6.3	3.1	4.9	3.1
TBSTA30-11	(275)	26.2	18.5	17.1	14.0	11.9	3.7	2.3	3.9	2.5
GEJOB01	(20)	15.8	22.6	17.0	12.7	11.3	4.5	3.8	7.2	5.2
GEJOB02	(50)	14.1	17.5	19.7	14.6	13.8	5.0	2.6	7.2	5.6
SVILL2-01	(20)	6.7	16.8	15.4	9.8	9.6	5.1	7.3	17.0	12.3
SVILL2-04	(65)	23.6	17.7	15.3	10.2	9.1	3.4	3.5	7.9	9.3
SVILL2-07	(100)	23.7	19.1	15.5	11.4	10.5	4.1	2.7	6.3	6.7
SPEN1-01	(20)	13.4	18.1	14.0	9.3	7.4	3.0	5.9	14.0	14.8
SPEN1-04	(65)	27.2	18.2	14.5	11.1	10.5	3.8	3.2	6.3	5.3
SPEN1-09	(110)	35.8	18.3	12.0	8.4	7.8	3.1	3.1	6.9	4.5

**APPENDIX B- 4.** Soil hydraulic properties for soil classes.

<b>CLASS 10</b>		<b>Regolith</b>								
<b>COD</b>	<b>DESC</b>	<b>XUTMW</b>	<b>YUTMW</b>	<b>ELEV</b>	<b>SOILtx</b>	<b>KC</b>	<b>FC</b>	<b>WP</b>	<b>POR</b>	<b>BETA</b>
LMAL03	Los Malones	735460	4548868	802	Sandy Loam	1405.7	15.2	5.9	44.1	3.3
TB05B1	Trabadillo La Mata	739657	4555673	751	Sandy Loam	1602.7	13.8	4.7	44.5	2.6
TB06B1	North boundary of La Mata	739652	4555749	743	Sandy Loam	772.3	19.5	9.9	43.1	4.9
GEJOR01	Gejo de los Reyes	736383	4555557	764	Sandy Loam	1179.2	16.7	7.0	43.9	3.7
TRABSS	Trabadillo near Albarranes	738522	4556380	755	Sandy Loam	798.8	19.9	8.5	43.8	4.5
GEJOB	Gejuelo del Barro	739479	4551461	798	Sandy Loam	1432.0	13.9	5.0	44.4	2.7
Svilo02	Via Villosino	740348	4555212	762	Sandy Loam	790.8	18.6	7.4	43.9	3.8
SPEN01	Penalbo Tanvir	737324	4553383	774	Sandy Loam	728.3	19.1	6.7	44.2	3.4
Mu-Hill	Mulledes-Hill	739009	4547539		Sandy Loam	1538.9	10.9	4.0	39.8	3.4
Gejo	Gejo	736088	4557843		Sandy Loam	1801.0	10.1	2.7	39.6	3.3
GjDB	Gejuelo Del Barro	741427	4551615		Loam Sand	2146.8	8.4	2.5	40.2	2.9
Trb-pyr	Trabadillo -Pyrenica	739473	4555923		Sandy Loam	749.0	15.6	7.7	38.7	4.5
Trb-ilx	Trabadillo- Ilex	739552	4555919		Loamy Sand	1578.5	10.0	4.4	39.7	3.2
Mu-AD	Mulledes-ADAS	738705	4547893		Loam	225.8	24.0	13.3	39.4	6.8
PNB-W-P	Penalbo-W-Pond	737844	4554714		Loamy Sand	2371.9	7.5	2.6	41.0	2.6
Trm-W	Tremedal-West	734341	4550840		Sandy Loam	1138.8	13.1	5.3	39.3	3.9
Average						1266.3	14.769	6.100	41.850	3.719
<b>CLASS 20</b>		<b>Regolith/Rock</b>								
		<b>20.00</b>								
<b>COD</b>	<b>DESC</b>	<b>XUTMW</b>	<b>YUTMW</b>	<b>ELEV</b>	<b>SOILtx</b>	<b>KC</b>	<b>FC</b>	<b>WP</b>	<b>POR</b>	<b>BETA</b>
TREM01	Tremedal	737291	4551392	763	Sandy Loam	1856.9	13.3	4.7	44.7	2.8
Sar-vlg	Sardon Village	736455.00	4548680.00		Sandy Loam	1449.6	10.9	4.5	39.4	3.4
PNB-WW	Penalbo WW	736145.00	4553805.00		Sandy Loam	895.7	14.5	6.5	38.8	4.3
Average						1400.7	13	5	41	3.500
<b>CLASS 3</b>		<b>Aluvium</b>								
		<b>30</b>								
<b>COD</b>	<b>DESC</b>	<b>XUTMW</b>	<b>YUTMW</b>	<b>ELEV</b>	<b>SOILtx</b>	<b>KC</b>	<b>FC</b>	<b>WP</b>	<b>POR</b>	<b>BETA</b>
TBSTA30	Trabadillo near station	739368	4555676	750	Sandy Loam	1325	15.6	4.8	44.5	2.7
PNB-S	Penalbo S	738430.00	4553560.00		Loamy Sand	2191.68	8.2	2.5	40.3	2.8
Trm	Trmedal (piezometer)	737070.00	4551350.00		Loamy Sand	2686.8	6.8	1.8	41	2.5
Average						2067.9	10	3	42	2.667

## APPENDIX C

### APPENDIX C- 1. Creation of classes for Vegetation map

Following steps were done using Excel spreadsheet:

- All the possible combinations among percentages multiples of fives were created with the respective values from three columns named: **Ilex**, **Pyrenaica** and **S+G** (Soil+Grass) See table below.
- In the columns % Rel <sub>Ilex</sub> and %Rel <sub>Pyrenaica</sub> the relative weights for each class was calculated with the formulas: %Rel<sub>Ilex</sub> = (%Ilex)/(%Ilex+%Pyrenaica); %Rel<sub>Pyrenaica</sub> = (%Pyrenaica)/(%Ilex+%Pyrenaica).

Table 10. Example of segmentation of vegetation classes

Classes	%Ilex	%Pyrenaica	S+G	Total	%Rel <sub>Ilex</sub>	%Rel <sub>Pyrenaica</sub>
1	000	000	100	100	0.0	0.0
2	005	000	095	100	1.0	0.0
3	010	000	090	100	1.0	0.0
4	015	000	085	100	1.0	0.0
5	020	000	080	100	1.0	0.0
.	.	.	.		.	.
.	.	.	.		.	.
.	.	.	.		.	.
230	005	095	000	100	0.05	0.95
231	000	100	000	100	0.0	1.0

- Properties as Root density (DENS1, DENS2,..., DENS6) for the mixed classes were calculated by weighted average of the estimated values of the simple species Q.Ilex, Q. Pyrenaica. For instance in the table below, in the case of a combination of Ilex50%-Pyrenaica5%, the variable DENS3 is calculated with the formula **dens3** <sub>Ilex50-Pyrenaica5</sub> = (Q.Ilex DENS3\* %Rel <sub>Ilex</sub>) + (Q.PyrenaicaDENS3\* %Rel<sub>Pyrenaica</sub>); Thus **dens3** <sub>Ilex50-Pyrenaica5</sub> = (50\*0.9) + (70\*0.1) = 51.8

Table 11. Sample of root density estimation

		DENS 1	DENS 2	DENS 3	DENS 4
	Q.Ilex	90	90	50	30
	Q.Pyrenaica	90	90	70	30
Total %	VegClass	dens1	dens2	dens3	dens4
45	Ilex40-Pyrenaica5	90	90	52.2	30
50	Ilex45-Pyrenaica5	90	90	52.0	30
55	Ilex50-Pyrenaica5	90	90	51.8	30
60	Ilex55-Pyrenaica5	90	90	51.7	30
65	Ilex60-Pyrenaica5	90	90	51.5	30



## APPENDIX D

---

### APPENDIX D- 1. List of main inputs and outputs files.

<b>File type</b>	<b>File name</b>
Input files	
Batch Control	infil3.ctl
Simulation Control	sardon.ctl
Geospatial Watershed Characteristics	sardon.gwc
Soil Properties	sardon.soils
Bedrock Properties	sardon.bedrock
Vegetation Properties	sardon.veget
Climate-Station Information	sardon.daystations
Monthly Climate-Regression Models	sardon.monthmod
Monthly Atmospheric Parameters	sardon.atmos
Daily Precipitation	sardon.precip
Daily Maximum Air Temperature	sardon.tmax
Daily Minimum Air Temperature	sardon.tmin
Output files	
Summary Output	sardon.outfile
Grid-Cell Properties	sardon.spatialout
Daily Output for all Grid Cells	sardon.daymap
Daily Output for Specific Grid Locations	sardon.point1, sardon.point2, sardon.point3, sardon.point4, sardon.point5, sardon.point6
Annual and Average Annual Output for all Grid Cells (prefix is "sardon")	sardon.0001, sardon.0002, sardon.0003
Crash File	sardon.crashfile
Spatially Averaged Daily Output	sardon.dayall
Monthly and Annual Output for all Grid Cells	sardon.outmonth, sardon.outannual
Average Annual Output for all Grid Cells During a Specified Averaging Period	sardon.flxfl